NEUROSCIENCE
RESEARCH ARTICLE
M. Ben Yakir-Blumkin et al. / Neuroscience 425 (2020) 217–234

Static Magnetic Field Exposure *In Vivo* Enhances the Generation of New Doublecortin-expressing Cells in the Sub-ventricular Zone and Neocortex of Adult Rats

Moriya Ben Yakir-Blumkin,[a] Yelena Loboda,[a] Levi Schächter[b] and John P. M. Finberg[a]*

[a] *Neuroscience Department, Rappaport Faculty of Medicine, Technion – Israel Institute of Technology, Haifa, Israel*

[b] *Department of Electrical Engineering, Technion – Israel Institute of Technology, Haifa, Israel*

Abstract—Static magnetic field (SMF) is gaining interest as a potential technique for modulating CNS neuronal activity. Previous studies have shown a pro-neurogenic effect of short periods of extremely low frequency pulsatile magnetic fields (PMF) *in vivo* and pro-survival effect of low intensity SMF in cultured neurons *in vitro*, but little is known about the *in vivo* effects of low to moderate intensity SMF on brain functions. We investigated the effect of continuously-applied SMF on subventricular zone (SVZ) neurogenesis and immature doublecortin (DCX)-expressing cells in the neocortex of young adult rats and in primary cultures of cortical neurons *in vitro*. A small (3 mm diameter) magnetic disc was implanted on the skull of rats at bregma, producing an average field strength of 4.3 mT at SVZ and 12.9 mT at inner neocortex. Levels of proliferation of SVZ stem cells were determined by 5-ethynyl-2′-deoxyuridine (EdU) labelling, and early neuronal phenotype development was determined by expression of doublecortin (DCX). To determine the effect of SMF on neurogenesis in vitro, permanent magnets were placed beneath the culture dishes. We found that low intensity SMF exposure enhances cell proliferation in SVZ and new DCX-expressing cells in neocortical regions of young adult rats. In primary cortical neuronal cultures, SMF exposure increased the expression of newly generated cells co-labelled with EdU and DCX or the mature neuronal marker NeuN, while activating a set of pro neuronal bHLH genes. SMF exposure has potential for treatment of neurodegenerative disease and conditions such as CNS trauma and affective disorders in which increased neurogenesis is desirable.

Key words: static magnetic field, neurogenesis, sub-ventricular zone, neocortex, primary neuronal culture.

INTRODUCTION

The production of new neurons in the hippocampal dentate gyrus (DG) and sub-ventricular zone (SVZ) of the mammalian brain persists into adulthood (Alvarez-Buylla and Garcia-Verdugo, 2002; Eriksson et al., 1998). The newly generated neurons stream towards the hippocampal DG and olfactory bulb (OB), respectively, where they differentiate into interneurons that integrate into the local neuronal networks. Although their functional importance in humans is somewhat elusive, neurons generated in adulthood are presumed to have a role in physiological brain functions such as hippocampal and olfactory learning and memory processes (Malvaut and Saghatelyan, 2016; Vivar and van Praag, 2013; Marin-Burgin and Schinder, 2012; Zhao et al., 2008). Moreover, neuronal precursors generated *in situ* in these regions in adulthood are suggested to have a role in the brain's response to acute neurological disorders such as ischemia (Marti-Fabregas et al., 2010; Jin et al., 2006; Macas et al., 2006; Jin et al., 2001), epilepsy (Parent et al., 2002) and traumatic brain injury (Dash et al., 2001), where a neurogenic response in the canonical neurogenic regions is up-regulated (Ohira et al., 2010; Nakatomi et al., 2002).

Perturbed neurogenesis in adulthood was associated with neuropsychiatric disorders such as schizophrenia

*Corresponding author.
E-mail address: finberg@technion.ac.il (J. P. M. Finberg).

Abbreviations: AD, Alzheimer's disease; ANOVA, analysis of variance; bHLH, basic helix-loop-helix; BrdU, 5-bromo-2′-deoxyuridine; BSA, bovine serum albumen; CC, corpus callosum; Cg1, cingulate cortex area 1; Cg2, cingulate cortex area 2; DAPI, 4′,6-diamidino-2-phenylin dole; DCX, doublecortin; DG, dentate gyrus; DIV, day *in vitro*; DMSO, dimethyl sulfoxide; EDTA, ethylene diamine acetic acid; EdU, 5-ethynyl-2′-deoxyuridine; ELFMF, extremely low frequency magnetic field; FCS, fetal calf serum; IQR, inter-quartile range; M1, primary motor cortex; M2, secondary motor cortex; MF, magnetic field; NBM, neurobasal medium; NeuN, neuronal nuclei; NSC, neuronal stem cell; OB, olfactory bulb; OPC, oligodendrocyte precursor cell; PCR, polymerase chain reaction; PD, Parkinson's disease; PSA-NCAM, polysialylated neural cell adhesion molecule; RMS, rostral migratory stream; ROI, region of interest; RSA, retrosplenial agranular cortex; RSGb, retrosplenial granular b cortex; RT, room temperature; SD, standard deviation; SEM, standard error of the mean; SMF, static magnetic field; SVZ, sub-ventricular zone; VGCC, voltage-gated calcium channel; WM, white matter.

https://doi.org/10.1016/j.neuroscience.2019.11.005
0306-4522/

and depression (Eriksson, 2006; Duman, 2004; Santarelli et al., 2003). Alterations in adult neurogenesis were also implicated in the pathogenesis of neurodegenerative diseases, where in addition to a massive, gradual loss of distinct neuronal populations, the innate capacity of cell renewal in adulthood is impaired (Reviewed by Winner and Winkler, 2015). For instance, reduced SVZ neurogenesis was detected in Alzheimer's disease (AD) and Huntington's disease animal models (Kandasamy et al., 2015), and in postmortem AD patients' brains (Ziabreva et al., 2006). However, although a decreased number of proliferating progenitors in the SVZ and OB was detected in a limited series of Parkinson's disease (PD) patients' brains (Hoglinger et al., 2004), and impaired proliferation and survival of newly born neurons were observed in animal models of PD (Marxreiter et al., 2013; Winner et al., 2011), there was no evidence for reduced SVZ proliferation rate of neuronal progenitors in a larger study of PD patients' brains (Van den Berge et al., 2011).

In recent decades, endogenous neuronal stem cells (NSCs) and precursor cells residing in different regions of the adult brain (Gage, 2000; Reynolds and Weiss, 1992) have emerged as a potential avenue to cell replacement therapy in neuronal loss conditions caused by different pathologies or brain injury (Kazanis, 2012). Therefore, much effort is invested in identifying stimuli capable of manipulating precursor cells in the adult brain and promoting adult neurogenesis within, and also outside, the canonical neurogenic niches. For instance, the possibility of stimulating neurogenesis in the neocortex, a region in which the existence of physiological neurogenesis in adulthood is highly debatable, is appealing due to its brain repair potential in conditions involving cortical neuronal loss, such as brain injury or AD, a progressive neurodegenerative disease and the most common cause of dementia in the elderly which contributes to 60–70% of 47.5 million dementia cases worldwide (World Health Organization, 2017).

In addition to a complex multifactorial endogenous regulation, multiple steps of adult neurogenesis such as cell proliferation, maturation and survival are responsive to environmental cues such as enriched environment, physical activity, stress (Zhao et al., 2008; Van Praag et al., 1999) and magnetic fields (MFs) exposure (Podda et al., 2014; Cuccurazzu et al., 2010; Piacentini et al., 2008; Arias-Carrion et al., 2004). MFs consist of a non-ionizing electromagnetic radiation that passes through and interacts with biological tissues (Rosen, 2003), thereby affecting key biological processes in various biological systems, including the CNS. In particular, 50–60 Hz Extremely Low Frequency MFs (ELFMFs) generated from power lines and household electric appliances in most European countries, and which are extensively studied due to their controversial epidemiological association with public health hazards (Eichholz, 2002; Kheifets et al., 1995), were shown to affect SVZ neurogenesis in nigrostriatal-lesioned rats (Arias-Carrion et al., 2004) and hippocampal neurogenesis in mice (Cuccurazzu et al., 2010), and to promote neuronal differentiation of postnatal mouse neuronal stem cells (Piacentini et al., 2008). In this study, we focus on low intensity static magnetic fields (SMFs), which have raised much interest in recent decades due to their therapeutic potential demonstrated in various biological systems, including the CNS (for example, see Miyakoshi, 2005; Saunders, 2005; Carter et al., 2002). Unlike ELFMFs, which are time varying, oscillating fields with frequencies below 300 Hz that generate electric currents upon interaction with charged particles in motion within the biological tissue, SMF are time independent fields that exert mechanical forces on charged particles and macromolecules but do not induce electric currents (Rosen, 2003). SMFs interact with cellular segments such as the cell membrane, susceptible to MFs due to the diamagnetic anisotropy property of its phospholipids (Worcester, 1978), thereby inducing biological alterations in membrane ion flux and ion channel kinetics (Rosen, 2003; Rosen, 1996). Nakamichi and colleagues (Nakamichi et al., 2009) found enhanced neurogenesis accompanied by alterations in expression of a variety of genes related to neuronal differentiation and survival as well as morphological changes in microspheres of rat neural progenitor cells exposed to 100 milliTesla (mT) SMF (note: 1 Tesla = 10,000 Gauss). The same strength SMF affected NMDA receptor channels and $Ca++$ levels in isolated rat hippocampal cells (Hirai et al, 2005). A higher strength SMF (300 mT) has recently been found to enhance differentiation of oligodendrocyte precursor cells *in vitro* (Prasad et al., 2017). A non-invasive 150–200 mT transcranial SMF stimulation was found safe in healthy human subjects while modulating cortical electrical activity (Oliviero et al., 2015).

Exposure of primary cortical neuronal cultures to SMFs affects gene expression and protects the neurons against neurotoxin-induced apoptosis, a specific mode of cell death associated with neurodegenerative diseases (Ben Yakir-Blumkin et al., 2014; Tenuzzo et al., 2009; Hirai and Yoneda, 2005). However, despite the beneficial effects induced by SMF *in vitro*, and in face of scarcity of an adequate experimental model for SMF exposure *in vivo* that enables a well-controlled and steady level of magnetic exposure, little is known about the biological effects exerted by low intensity SMF exposure in the CNS *in vivo*. In particular, neuroprotection and neurogenesis stimulation in the adult brain by SMF exposure remains largely unstudied. We are interested in the effects of low strength SMF, following our previous observations of a neuroprotective effect of 5 mT SMF in primary rat cortical cells (Ben Yakir-Blumkin et al., 2014), and in the present study we describe an *in vivo* model that assures a constant SMF exposure over time in the adult rat by implantation of a 3 mm diameter magnetic disc, which was attached to the skull and positioned above bregma (shown in Fig. 1A). Providing an accurate and steady mode of an average ± SEM 4.3 ± 0.23 mT to 12.9 ± 0.66 mT exposure in the desired anatomical regions, this model enabled us to study the effect of this low to moderate level SMF exposure on DCX^+/EdU^+ neuroblast generation in the SVZ and the neocortex, without the need to immobilize the animals for application of the magnetic field, and limiting magnetic field exposure to the animal's head. We found that exposure of young

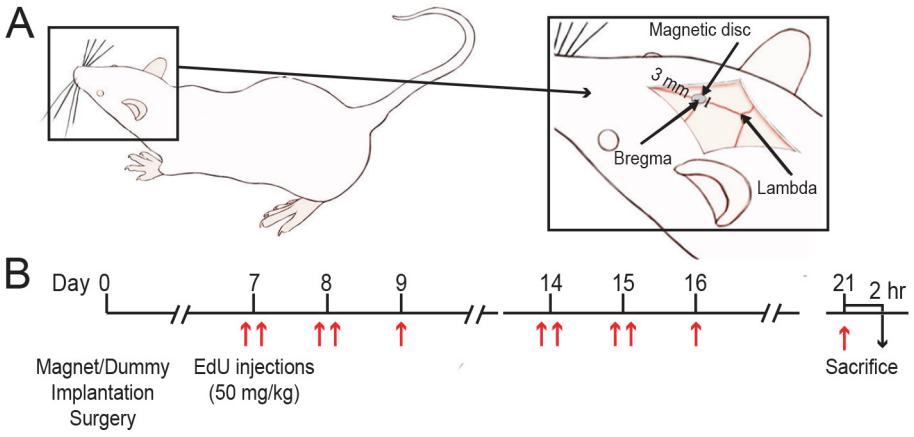

Fig. 1. *In vivo* experimental procedure. (**A**) A 3 mm diameter (0.65 mm thick) Ti-coated magnet or non-magnetic Ti-coated metal disc (sham-exposure) was attached to the rat's skull at bregma with a bio-glue surgical adhesive. Seven and 8 days post-surgery, rats received 2 i.p. injections of 5-ethynyl-2′-deoxyuridine (EdU, 50 mg/Kg per injection, at 10:00 am and 2:00 pm, as indicated by the red arrows in B), followed by a single i.p. injection the next day (10:00 am). This regime was repeated after a 7-day interval, and rats were sacrificed 21 days post implantation, 2 h after a final EdU injection (**B**). Sham control rats were implanted with an identical disc but made of non-magnetic material (dummy). Naïve rats were not operated or implanted. The EdU regime was the same for all 3 experimental groups.

adult rats to SMF caused an increase in SVZ cell proliferation and neurogenesis, and resulted in the stimulation of DCX^+/EdU^+ cell generation in the neocortex, a region severely affected during the course of neurodegenerative diseases and brain trauma. In primary cortical neurons, SMF exposure increased the expression of early- and late-phase neuronal markers by newly generated EDU^+ cells, activating a set of pro-neuronal bHLH genes that support neurogenesis. Altogether, our study provides indication to a possible pro-neurogenic activity of low-intensity SMF exposure *in vivo* and *in vitro*.

EXPERIMENTAL PROCEDURES

Unless otherwise specified, all reagents and chemicals were purchased from Sigma-Aldrich (St. Louis, MO).

Animal procedures

All procedures with animals were authorized by the Technion's Animal Care and Use Committee, whose ethical standards are based on those detailed in the National Institutes of Health (Bethesda, MD) Guide for the Care and Use of Laboratory Animals (NIH Publications No. 80-23, revised 1996), and whose general procedures for animal welfare comply with Israeli law on animal experimentation.

Magnetic disc surgical implantation procedure

15 Male SD rats (weighing 300 ± 20 g, Envigo, Jerusalem, Israel) were used for this study. The design of the study included 3 experimental groups: Naïve (not operated, no implant), SMF-exposed and Sham control (non-magnetic disc-implanted) rats.

The rats were acclimated to the housing conditions for 7 days, after which they were deeply anesthetized with an i.p injection of Ketamine (90 mg/Kg) and Xylazine (10 mg/Kg) and placed in a stereotactic frame. The hair in the relevant scalp area (above bregma) was removed and the skin was sterilized with Polydine solution. A 15 mm dorsal incision was made, followed by the removal of all soft tissues. A 3 × 0.65 mm (diameter and thickness) titanium (Ti)-coated magnet or Ti-coated non-magnetic metal disc (dummy) was attached to the skull (on bregma, see Fig. 1A for details) using cyanoacrylate surgical adhesive. The magnetic field strength on the surface of the magnetic disc measured using a Gauss-meter equipped with a Hall probe (Hirst Magnetic Instruments Ltd., Cornwall, UK) was 70 mT and decreased rapidly with distance from the surface to an average calculated value of 12.9 ± 0.66 mT (±SEM) at inner neocortex, and 4.3 ± 0.23 mT SMF intensity in the SVZ area, as detailed in Table 1. The calculation of the magnetic field strengths generated by the permanent magnet is shown after the Discussion section. After surgery, rats were administered a single dose of the non-steroidal anti-inflammatory drug Carprofen (5 mg/Kg, s.c.) for pain relief.

Magnetic field intensity (mT) at the co-ordinates from bregma shown in the table was calculated using the equation shown at the end of the Discussion.

EdU labeling and tissue processing for immunohistochemistry

To label dividing cells in the SVZ and neocortex, commencing 7 days post-surgery, all animal groups

Table 1. SMF intensity in the neocortex and SVZ

SVZ: rostral (+) or caudal (−) (mm)	Lateral (mm)	Ventral (mm)	mT
+1	1	4	3.5
+0.7	1	4	3.6
+0.5	1	3.5	4.8
+0.2	1	3.5	4.9
−0.26	1	3.5	4.9
−0.4	1	3.5	4.9
−0.8	1.5	3.5	4.3
−1.3	2	3.5	3.6
Cortex: rostral (+) or caudal (−)	**Lateral (mm)**	**Ventral (mm)**	**mT**
−1.4	1	1.5	15.1
−1.6	1	1.5	13.9
−1.8	1	1.5	12.6
−1.9	1	1.5	12.0
−2.1	0.8	1.5	11.4

were administered 5-ethynyl-2′-deoxyuridine (EdU, Invitrogen, Carlsbad, CA, USA), a tracer molecule that is incorporated into DNA of dividing cells during the cell cycle synthesis phase, and is subsequently detected by immunohistochemistry.

EdU was freshly dissolved in pre-warmed saline solution containing 0.1% DMSO and 0.0014% NaOH. In order to maximize the number of proliferating cells labeled by EdU across the entire study period (21 days), and given the limited bioavailability of thymidine analogs for s-phase cell labeling post injection (Hayes and Nowakowski, 2000), we used a multiple EdU injection regime (Thomas et al., 2007), in which rats received 2 daily EdU injections (50 mg/Kg, i.p.) for 2 days, followed by a single injection the next day. The injection regime was repeated after a 7-day interval, as depicted in Fig. 1B. Twenty-one days post implantation, rats were administered a final dose of EdU, and 2 h later were terminally anesthetized with ketamine/xylazine, then perfused transcardially with heparinized phosphate-buffered saline (PBS) followed by paraformaldehyde (4% w/v in PBS). Brains were removed, and the SVZ (+1.6 mm to −1.3 mm) or cortex (−1.5 mm to −2.12 mm) with respect to bregma (Paxinos et al., 1985) were sectioned into 40 μm free-floating sections, and stored in an anti-freeze solution (25% glycerol, 25% ethylene glycol in PBS) at 4 °C.

Immunostaining of SVZ and neocortical sections

The detection of EdU, DCX and s100β labeled cells was achieved via immunofluorescent staining. For the detection of EdU^+ cells, free-floating SVZ and neocortical sections were permeabilized with 0.5% Triton in PBS, blocked with 2% BSA in PBS for 10 min., and reacted with Alexa Fluor 555 conjugated azide (1 μM) that forms a covalent bond with the alkyne group in the EdU molecule incorporated into DNA, via click chemistry (Click-it EdU kit, Invitrogen, Carlsbad, CA, used according to manufacturer's instructions). For the detection of DCX, s100β, or NeuN, EdU-stained sections were subsequently washed with 2% BSA in PBS, blocked for 1 h at room temperature (RT) (blocking solution: 3% FCS, 1% BSA, 0.3% Triton in PBS) and incubated with goat anti-DCX primary antibody (1:500, Santa Cruz, Dallas, Texas), mouse anti-s100β (1:200, Sigma-Aldrich, Israel), or mouse anti-NeuN, (1:500, Merck, CA) for 16 h at 4 °C. Sections were then washed with PBS and incubated with a secondary antibody (Alexa Fluor 488 donkey anti-goat, 1:200, Alexa Fluor 647 donkey anti-mouse, 1:100, or Alexa Fluor 488 goat anti mouse,1:500, Invitrogen) for 1 h at RT. SVZ sections were further washed and mounted in a DAPI-containing mounting solution (Vectashield, Vector laboratories, Burlingame, CA). Neocortical sections were incubated with 33342-Hoechst dye (1:10,000) during the secondary antibody incubation, and mounted with DAPI-free mounting solution (Vectashield) on Superfrost Plus microscope slides (ThermoFisher Scientific, Waltham, MA, USA).

Confocal microscopy data acquisition of DCX, NeuN and EdU in brain sections

SVZ: To sample the SVZ, a total of 8 bilateral SVZ sections (+1.00, +0.70, +0.48, +0.20, −0.2, −0.4, −0.8 and −1.30 mm relative to bregma) spanning a 5.8 mm^3 bilateral volume of the SVZ in each animal were scanned in a confocal microscope and analyzed (n = 5 rats in each experimental group).

Neocortex: Five bilateral coronal sections per rat at −1.50, −1.60, −1.80, −1.90 and −2.12 mm relative to bregma were collected, and a total cortical volume of 3.1 mm^3 (bilateral ROI of 5.00 mm^2 multiplied by 0.62 mm depth), covering the M1, M2, cingulate 1, cingulate 2 regions, was sampled in each of n = 5 rats in each experimental group.

SVZ and neocortical sections were scanned using an LSM 700 laser scanning confocal system attached to an upright motorized microscope (Axio Imager.Z2, Carl Zeiss microscopy, Jena, Germany), equipped with X40/1.3-NA EC Plan Neofluar or X25/0.8-NA LD LCI Plan Apochromat oil immersion objective lenses and photo-multiplier tube detectors. To verify the co-localization of DCX/ EdU/Hoechst 33342 or NeuN/EdU/DAPI in the same cell, all images were acquired in a series of z-axis stacked images, captured at 1024 × 1024 (SVZ, 12 z-sections of 1.60 μm) or 512 × 512 (cortex, 12 z-sections of 1.16 μm) pixel resolution using the Zen 2010 software (Zeiss, Jena, Germany). For NeuN/EdU/DAPI quantification and co-localization analysis, 5 bilateral neocortical sections per each animal (n = 5 in each group) were scanned using a Panoramic MIDI automatic digital slide scanner system (3DHistech Ltd., Budapest, Hungary) equipped with a Plan-Apochromat x 20/0.8 objective lens attached to a monochrome camera (AxioCam MRm, Zeiss, Germany). Each image was obtained as a 10 z-section stack (1 μm intervals), and subjected to a 3D cell-by-cell analysis using the Imaris software 7.14 (Bitplan, Zurich, Switzerland). Dying cells with abnormal nuclear morphology exhibiting apoptotic Hoechst-33342 fluorescent emission and which may express cell cycle markers were excluded from the analysis.

In vivo data analysis

3D analyses of all images included the counting of EdU^+, DCX^+ and EdU^+/DCX^+ cells by a blind-to-treatment investigator. Co-localization analysis was accomplished in the following manner: each of the z-stack confocal images of SVZ and cortex was subjected to the following spots and surfaces analysis using Imaris software; EdU and DAPI or Hoechst 33342 labels were separately modeled as spots with a diameter based on the average of 50 labeled cells from each group. True $EdU^+/DAPI^+$ or $Hoechst^+$ co-localizing cells were first filtered, and false positive cells were excluded from the analysis at this stage. In the next step, DCX label in every cell was modeled as a surface. We then applied a "spots close to surfaces" calculating function, which calculated the number of the spots that are $EdU^+/DAPI^+$ or $Hoechst^+$ that are located within the center of

a given DCX surface. For $NeuN^+/EdU^+$ co-localization analysis, $EdU^+/DAPI^+$ cells were at first filtered as described above and represented as spots, followed by the modeling of NeuN cells as a second type of spots. Co-localization of the 2 spot types was determined by applying a suitable algorithm and verified by a 3D visualization of each co-localizing cell. We performed preliminary tests to verify the accurate identification of these cells as true positive cells, by comparing the algorithm's results with those obtained in a manual 3D count, resulting in less than 2.5% deviation between the two methods. Results were not multiplied by the sampling fractions, and reflect the actual numbers of cells in the analyzed sections.

Statistical analysis of *in vivo* data

For the SVZ, quantitative data was based on the average EdU^+, DCX^+, EdU^+/DCX^+ or $EdU^+/NeuN^+$ cell number in the 16 confocal SVZ images for each animal and the mean of $n = 5$ rats in each experimental group. For the neocortex, quantitative data was based on the average EdU+, DCX+, EdU+/DCX+ or EdU+/NeuN+ cell number in the 10 confocal images of the cortex per animal and the mean data from $n = 5$ rats in each experimental group. To determine the suitable statistical test, data were first analyzed for normal distribution using Shapiro–Wilk and Kolmogorov–Smirnov tests, and differences in SDs within relevant data sets were tested using the Brown–Forsythe test. All relevant data sets analyzed were found to be normally distributed with equal SDs. Statistical analyses were therefore carried out using one-way ANOVA, followed by Dunnet's post hoc test for multiple comparisons. All statistical analyses were done using GraphPad Prism 8.0 (GraphPad Software Inc. La-Jolla, CA). Data are presented as the mean ± SEM. Differences between treated cultures and controls were considered significant at p value < 0.05 (*), $p < 0.01$ (**), or $p < 0.001$ (***). Exact F(n,df) values are stated in the text.

In vitro experiments

Rat primary cortical neuronal preparation. Dissociated neurons were prepared from the brain cortices of postnatal day 1 Sprague-Dawley (SD) rats (Harlan laboratories, Jerusalem, Israel), plated on poly-D-lysine coated coverslips placed in 24-well plates ($2.5{\cdot}10^5$ cells/well) and maintained in Neurobasal Medium (NBM) supplemented with B27 (Gibco, Grand island, NY, USA) throughout the experiments.

SMF exposure system. SMF exposure was generated using an array of 24 (6×4) $Ne_2Fe_{14}B$ magnetic discs of 11.2 mm diameter and known intensity, placed below the 24-well culture plates (6×4) located in a 5% CO_2 and 37 °C incubator. The magnetic field intensity generated in the 24-well plate was mapped at 5 constant points in each well using a Gaussmeter (Hirst Magnetic Instruments Ltd, UK) equipped with a Hall probe. For immunohistochemistry experiments, cultures were exposed to 5 mT SMF for 7 days. On DIV7, data were collected from non-overlapping random fields in at least 3 wells per experimental condition. For real time PCR, cultures were exposed to 5 mT SMF on DIV5 for 72 h (until DIV7), and data were collected from a whole plate (24 wells) per experimental condition.

EdU and BrdU labeling: immunohistochemistry, data acquisition and 3D analysis. To label proliferating cells, SMF-exposed or control cultures were labeled with either the thymidine analogue 5-bromo-2′-deoxyuridine (BrdU), or 5-ethynyl-2′-deoxyuridine (EdU, Invitrogen), both selectively incorporated into synthesized DNA of newborn cells at their S-phase in cell cycle, and subsequently detected by immunohistochemistry. EdU was freshly dissolved with 0.1% DMSO and 0.0014% NaOH in a pre-warmed saline solution, and was added to the cultures (10 μM) on DIV2 and DIV6 during a 7-day experimental course. Alternatively, cultures were incubated on DIV2 and DIV6 with BrdU (10 μM). On DIV7, cells were fixed with 4% paraformaldehyde in PBS and permeabilized with 0.5% Triton in PBS. For the detection of EdU^+/DCX^+ and $EdU^+/NeuN^+$, cells were washed with 2% BSA in PBS, blocked for 1 h at RT (blocking solution: 3% FCS, 1% BSA, 0.3% Triton in PBS) followed by incubation with Alexa Fluor 555 nm conjugated azide (Click-it EdU kit, Invitrogen, used according to manufacturer's instructions). Cells were then reacted with either goat anti-DCX primary antibody (1:500, Santa Cruz, Dallas, Texas) or mouse anti-NeuN, (1:500, Merck, CA) for 16 h at 4 °C, washed with PBS and further incubated with the appropriate secondary antibody (DCX: Alexa Fluor 488 donkey anti goat, 1:200, NeuN: Alexa Flour 488 goat anti mouse, 1:500, Thermo-Fisher Scientific Inc.) for 1 h at RT.

For the detection of $BrdU^+/NeuN^+$ cells, following fixation and permeabilization, cells were blocked and incubated with sheep polyclonal anti-BrdU (1:400, Abcam, Cambridge, UK) and mouse anti-NeuN, (1:500) for 16 h at 4 °C, washed (0.1% Triton in PBS) and reacted with the secondary antibodies (BrdU: Alexa Fluor donkey anti-sheep 568 1:600, NeuN: Alexa Fluor 488 goat anti mouse, 1:500) for 1 h at RT. Nuclei were stained with Hoechst-33342 reagent. All staining combinations (EdU/DCX, EdU/NeuN, BrdU/NeuN) were visualized using an LSM 700 laser scanning confocal system attached to an upright motorized microscope.

To determine the co-localization of EdU with either DCX or NeuN in the same cell, 4 coverslips per experimental condition were scanned using a Panoramic MIDI automatic digital slide scanner system (3DHistech Ltd., Budapest, Hungary), equipped with a Plan-Apochromat x 20/0.8 objective lens attached to a monochrome camera (AxioCam MRm, Zeiss, Germany). Each image was obtained as a 10 z-section stack (1 μm intervals), and subjected to a 3D cell by cell analysis using the Imaris software, as described in the *in vivo*

data analysis methodology section. For quantification, data were sampled from 4 parallel wells per experimental condition. In each well, an ROI of 1500 × 1500 μm was scanned, and cell numbers in 2 non-overlapping regions (1500 × 750 μm each) in each well were counted by a blind-to-treatment investigator, averaged and presented as mean ± SEM. All experiments were repeated at least 3 times.

Real time quantitative PCR (qPCR) analysis

Cultures were sham- or SMF-exposed for 72 h (DIV5-DIV7). On DIV7, cells were thoroughly washed with ice cold PBS (3 times) and incubated with Trypsin/EDTA solution (0.25% Trypsin/EDTA, Biological Industries, Beit-Haemek, Israel) for 10 min at 37 °C. Cells were then scraped from wells and mRNA was extracted from a single 24-well plate per experimental condition. Total mRNA was isolated using a commercial kit according to manufacturer's instructions (5 Prime, Hilden, Germany). DNA was digested using on-column RNase-free DNase (5 Prime, Hilden, Germany). Following determination of nucleic acid concentration by nanodrop (ThermoFisher scientific Inc., Wilmington, DE, USA), RNA was reversed-transcribed to cDNA using a commercial kit (Applied Biosystems, Foster city, CA, USA), according to manufacturer's instructions. For qPCR, cDNA was reacted with Tacqman mix and primers of interest (Applied Biosystems), and samples were run in a 7500 real time PCR equipment (Applied Biosystems). Data were analyzed using the real time PCR 7500 software (Applied Biosystems, Life Technologies) and the fold change in gene expression was calculated using the $2^{-\Delta\Delta CT}$ method (Livak and Schmittgen, 2001). In each experiment, all samples were run in triplicates and normalized to the level of an endogenous house-keeping gene (GusB). The ensuing relative gene expression level of each gene was finally calculated relative to its expression value in the sham control cultures ($\Delta\Delta Ct = (Ct_{\text{selected gene}} - Ct_{\text{GusB}})_{\text{SMF-exposed group}} - (Ct_{\text{selected gene}} - Ct_{\text{GusB}})_{\text{sham group}}$). See Table 2 for details of the selected genes. At least 3 independent experiments were carried out to determine the change in expression of all the genes, and results are presented as the mean values ± SEM (for data analyzed by Student's *t*-test) or median values and interquartile range (IQR) (for data analyzed by Mann–hitney test).

Table 2. List of genes whose expression level was determined in primary neuronal cultures.

Gene	Gene Name	Gene Symbol	Ref. Sequence
GusB	Glucuronidase; beta	Gusb	NM_017015.2
Mash1	Achaete-scute complex homolog 1 (Drosophila)	Ascl1	NM_022384.1
NeuroD1	Neurogenic differentiation 1	Neurod1	NM_019218.2
NeuroD2	Neurogenic differentiation 2	Neurod2	NM_019326.1
Ngn1	Neurogenin 1	Neurog1	NM_019207.1

In vitro data statistical analysis

Independent primary neuronal cell preparations were used for each biological repetition. Statistical comparison between SMF-exposed and control cultures was carried out using unpaired Student's *t*-test (GraphPad Prism 8.0) for data sets which are normally distributed as tested by the Shapiro–Wilk test, and have equal SDs, or by *t*-test with Welch's correction without assuming equal SDs. Data are presented as mean ± SEM (for normally distributed data) or as median and IQR values (for non-parametric data). Differences between experimental groups were considered significant at $p < 0.05$ (*), $p < 0.01$ (**), $p < 0.001$ (***), and $p < 0.0001$ (****). Exact $t(n,df)$ values (for *t*-test) or $U(n1, n2)$ values (for Mann–Whitney test) are stated in the text.

RESULTS

SMF exposure stimulates cell proliferation and neuroblast generation in the adult SVZ *in vivo*

To study the effect of SMF exposure on cell proliferation and SVZ neuroblast generation, rats were subjected to a multiple injection regime of EdU (illustrated in Fig. 1B), a molecule that is incorporated into and labels the DNA of mitotically active cells that enter the cell cycle's s-phase (Buck et al., 2008). The expression of EdU and DCX, a migrating neuroblast marker abundant in the SVZ in adulthood, was quantitatively analyzed as described in Experimental Procedures section above. Four representative sections from SMF-exposed and Sham control rats are shown in Fig. 2A–D).

SMF exposure increased the number of EdU^+ proliferating cells residing in the same SVZ volume by 59.1%, compared with Sham control rats [SMF: 2838 ± 166.3, Sham control: 1783 ± 256, Naïve control: 2006 ± 276 cells; mean cell number ± SEM for $n = 5$ in each group, $p < 0.05$, for the difference between the 3 experimental groups, $F(2,12) = 5.477$, Fig. 2E]. Naïve rat's data are not presented in Fig. 2 in the interests of brevity. No significant differences occurred between Sham control and Naive groups. To examine whether the increase in cell proliferation in the SVZ in SMF-exposed rats reflects an increase in neuroblast generation, we further analyzed the number of DCX^+ and EdU^+/DCX^+ double positive cells in the different experimental groups. While the number of DCX^+ cells in SMF, Sham control and Naïve rats was not statistically different [SMF: 3558 ± 300.5, Sham control: 3134 ± 377.2, Naïve: 3018 ± 310; mean cell number ± SEM for $n = 5$ in each group, $p > 0.05$ for the difference between the 3 experimental groups, $F(2,12) = 0.737$, Fig. 2F], we observed a marked increase of 66.0% in the number of newly generated SVZ proliferating neuroblasts, co-labeled with both DCX and EdU in SMF-exposed rats, compared with Sham control rats [SMF: 1695 ± 172.1 cells, Sham control:1021 ± 116.4 cells, Naïve: 1187 ± 109.0 cells; mean cell number ± SEM for $n = 5$ in each group, $p < 0.05$ for the difference between the 3 experimental groups, $F(2,12) = 6.72$, Fig. 2G].

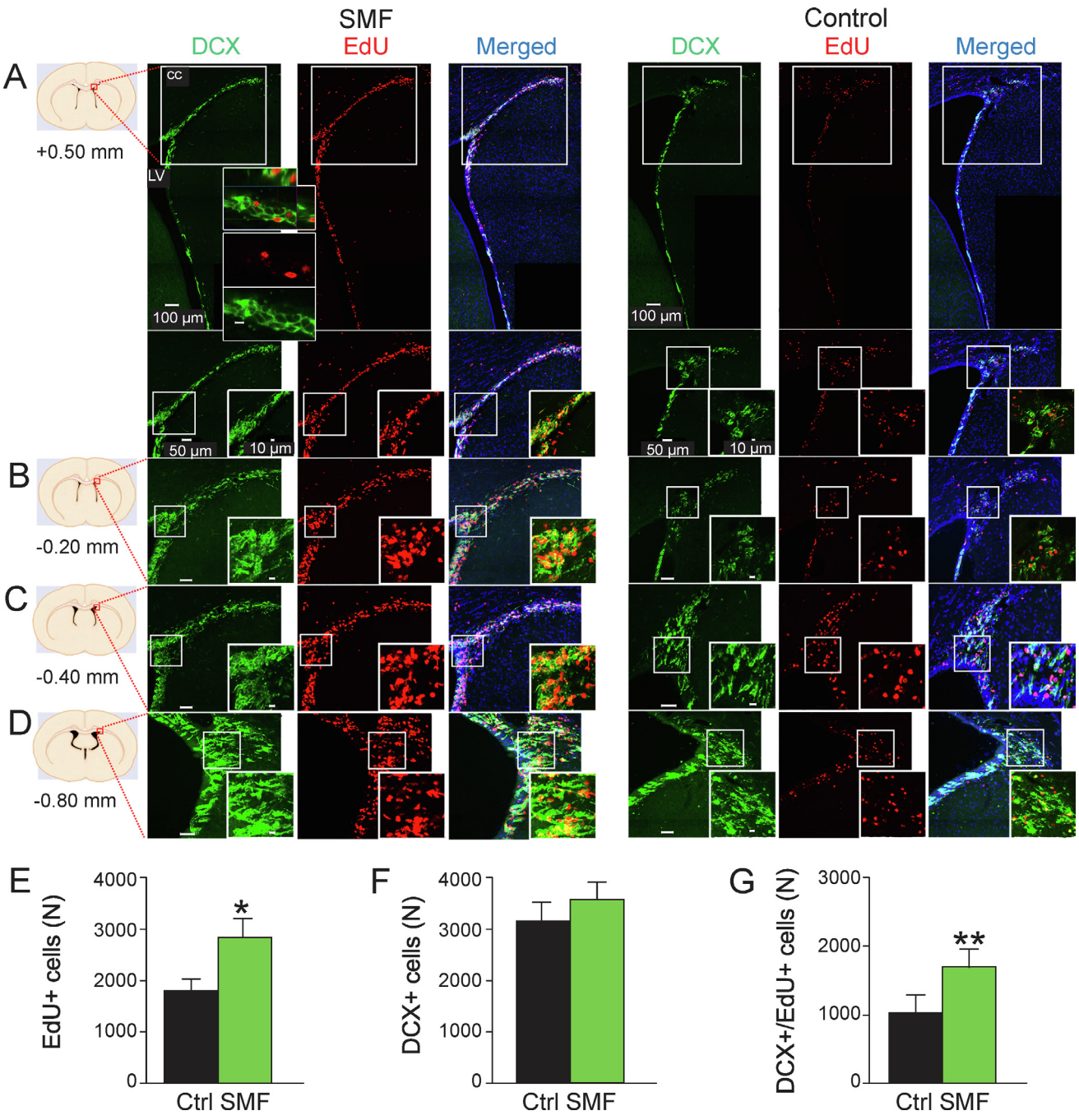

Fig. 2. Enhanced generation of SVZ neuroblasts in SMF-exposed adult rats. Representative confocal images of SVZ sections obtained from SMF- and Sham-exposed (control) rats, at +0.50 mm (**A**), −0.20 mm (**B**), −0.40 mm (**C**) and −0.80 mm (**D**) with respect to bregma, stained with fluorescent antibodies against DCX or EdU or with DAPI. Each confocal image represents a stack of 12 consecutive z-section images (1.60 µm). Analyses of 8 bilateral sections represented by 16 confocal images per rat and quantifications of cell numbers show an increase in EdU-incorporating cells in SMF-exposed rats (**E**, mean cell number ± SEM, for $n = 5$ in each group, $^{*}p < 0.05$), without a significant change in the number of DCX+ cells, compared with Sham control (**F**, mean cell number ± SEM for $n = 5$ in each group, $p > 0.05$). Co-localization analysis shows an increase in the total DCX^{+}/EdU^{+} cell number detected in the SVZ of SMF-exposed rats (**G**, mean cell number ± SEM for $n = 5$ in each group, $^{**}p < 0.01$) All data sets were analyzed using One-way ANOVA followed by Dunnet's post hoc test for multiple comparisons.

SMF exposure increases the expression of the immature neuronal marker DCX in EdU^{+} newly generated neocortical cells *in vivo*

We next examined whether a sub-population of newly generated DCX^{+} cells resides in the neocortex, a region referred to as non-neurogenic in adulthood, and in which neurons are severely affected during the course of AD, and whether SMF exposure increases its size. We analyzed the expression of DCX^{+} and DCX^{+}/EdU^{+} cells in a 5.00 mm^2 ROI measured bilaterally in rat neocortical sections from −1.50 mm to −2.12 mm (with respect to bregma), spanning a total neocortical volume of 3.1 mm^3

(0.62 mm depth multiplied by 5.00 mm^2 area in xy plane). Within the examined volume, pre-existing as well as newly-generated DCX^+/EdU^+ cells were detected throughout several neocortical sub-regions (M1, M2, Cg1, Cg2, RSA and RSGb), in all experimental groups, including Naïve rats (representative images of SMF-exposed and Sham control rats' sections are shown in Fig. 3). DCX^+/EdU^+ cells were in particular widespread in neocortices of rats exposed to SMF, as indicated in Fig. 3A, compared with the identical cortical regions in corresponding Sham-control rats, in which DCX^+/EdU^+ cells were sparsely distributed (Fig. 3B). Distribution of such cells in Naive rats was similar to Sham-control.

Unlike previous findings (Klempin et al., 2011; Shapiro et al., 2007; Pekcec et al., 2006; Nacher et al., 2001; Bonfanti et al., 1992; Seki and Arai, 1991) showing a distinct localization pattern of DCX^+ cells in layer II /III of the adult piriform- or neo-cortex, DCX^+ and DCX^+/EdU^+ cells detected in this study were dispersed throughout all neocortical layers, including the piriform cortex, and

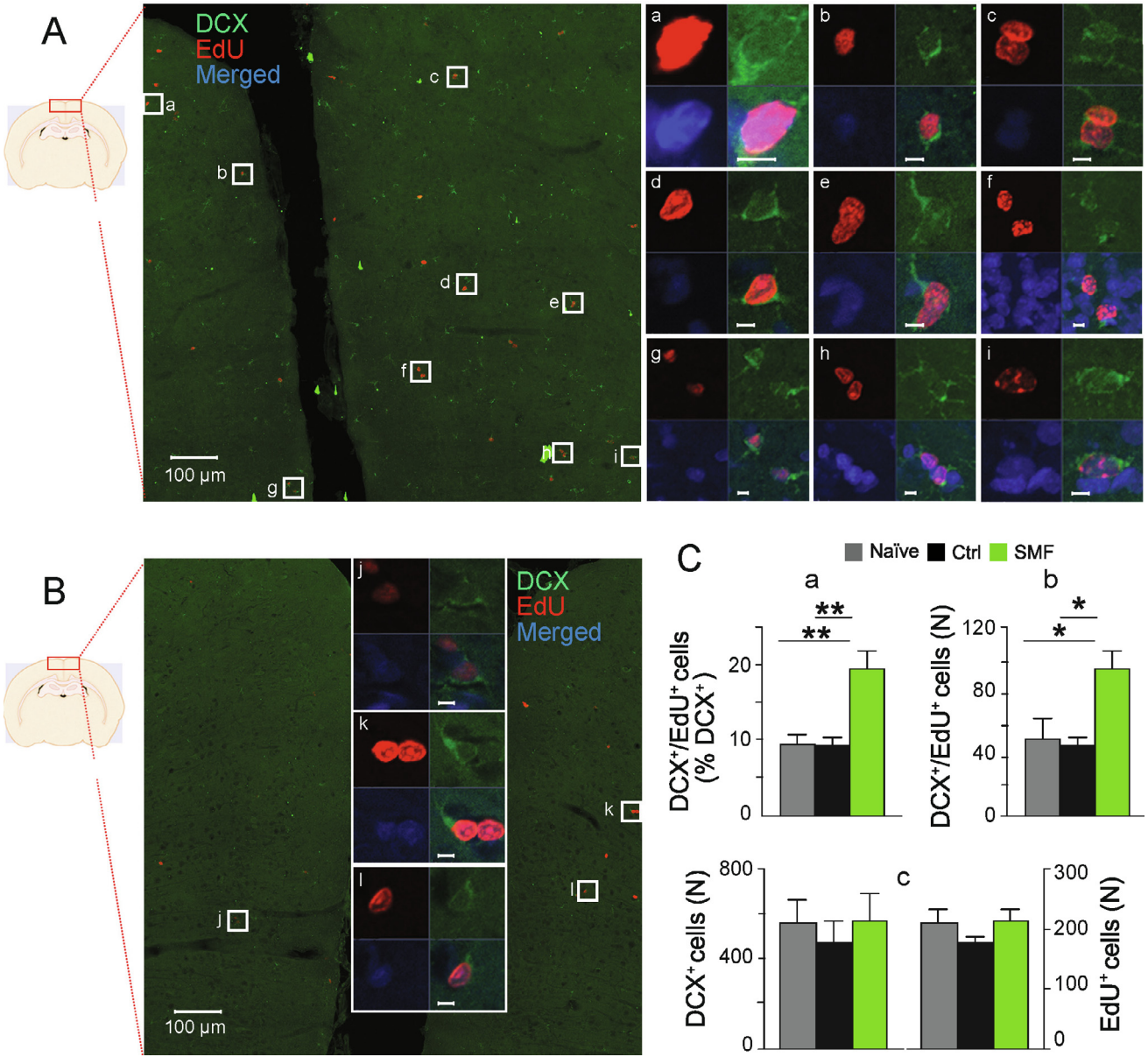

Fig. 3. Representative confocal images of neocortical brain sections (bregma −1.88 mm, area shown in (**A**) co-stained with antibodies against DCX and EdU and labeled with Hoechst-33342, showing the distribution of DCX^+/EdU^+ cells detected in SMF- (**A; a–i**) and Sham control-exposed rats (**B; j–l**). (**C**) Co-localization analyses of DCX/EdU co-labeled cells in the neocortex, based on 10 confocal images of 5 bilateral sections per rat, showing a constitutive generation of DCX^+/EdU^+ cells in Naïve (not operated) and Sham (dummy implant) control rats (Ctrl), which is enhanced in rats exposed to SMF. Mean percentage of DCX^+/EdU^+ cell number ± SEM for $n = 5$ in each group is presented in (**a**), and analyzed using One-way ANOVA followed by Dunnett's Post-hoc test. $^{**}p < 0.01$ (SMF vs. Sham control), $^{**}p < 0.01$ (SMF vs. Naïve). Mean DCX^+/EdU^+ cell number ± SEM for $n = 5$ in each group is presented in (**b**). Results of ANOVAs were significant at $^{*}p < 0.05$ (SMF vs. Sham control) and $^{*}p < 0.05$ (SMF vs. Naïve). Mean DCX^+ or EdU^+ cell numbers ± SEM for $n = 5$ in each group are presented in (c), multiple comparisons were insignificant (DCX^+ p values > 0.05 for SMF vs. dummy and SMF vs. Naïve, EDU^+ p values: > 0.05 for SMF vs. dummy, and SMF vs. Naïve).

deep cortical layers (Fig. 4, a–f), extending towards the WM and CC (Fig. 4, e, f), regions located adjacently to the SVZ. Many of these cells were mitotically active and detected as cell doublets (for example, see Fig. 3Bk), or in close proximity (less than 5 μm) to another DCX^+/EdU^+ cell (i.e., in Fig. 3Bf-h).

Quantifying the number of DCX^+/EdU^+ cells, we found that 9.3 ± 1.25% and 9.1 ± 1.03% of DCX^+ cells detected in the neocortex of Naïve and Sham control rats, respectively, were newly generated EdU^+ cells added in adulthood, implying a constitutive addition of new neocortical cells with neuronal potential during maturity (Fig. 3C). SMF exposure further stimulated the generation of these new immature DCX^+ cells, and doubled the number of cells co-expressing DCX and EdU residing in the identical neocortical volume, resulting in 19.3 ± 2.56% of DCX^+ cells co-labeled with EdU (mean percentage of cell number ± SEM for $n = 5$ in each group; $p < 0.01$ for the difference between the 3 experimental groups, $F(2,12) = 11.01$, Fig. 3C). We detected a total number of 91.8 ± 11.7 cells co-labeled with DCX and EdU in the examined sections in SMF-exposed group, compared with 48.4 ± 12.94 DCX^+/EdU^+ cells in the Naïve group, and 41.8 ± 8.40 cells detected in the Sham control group [mean cell number ± SEM for $n = 5$ in each group; $p < 0.05$ for the difference between the 3 experimental groups, $F(2,12) = 5.916$, Fig. 3C]. No significant change was observed in the number of DCX^+ cells [$p > 0.05$ for the difference between the 3 experimental groups, $F(2,12) = 0.5597$], nor was it evident in the number of EdU^+ proliferating cells [$p > 0.05$ for the difference between the 3 experimental groups, $F(2,12) = 0.2733$], as shown in Fig. 3C.

We also analyzed the expression of the glial marker s100ß by DCX^+/EdU^+ cells in a randomly selected neocortical brain section in the relevant bregma range in each rat ($n = 5$ in each experimental group). None of the cells co-labeled with DCX/EdU in the examined sections of all rats in all experimental groups co-expressed s100ß (Fig. 5), implying that these newly generated cells are not of glial lineage.

A low incidence of mature $Edu^+/NeuN^+$ neurons is found in the neocortex

We next analyzed the number of newly generated EdU^+ cells co-expressing the mature neuronal marker NeuN in a separate subset of brain sections obtained from the same co-ordinates. A slight trend to increase in SMF-exposed rats was observed in the fraction of EdU labeled cells co-expressing NeuN (mean ± SEM: 7.7 ± 2.28% in SMF-exposed mice, compared with 5.5 ± 1.92% and 4.9 ± 0.42% in the Sham-control and Naïve experimental groups, respectively). The total number of $NeuN^+/EdU^+$ cells was low, and no significant difference between the experimental groups was observed (18.8 ± 3.7 cells in SMF-exposed group, compared with 18 ± 6.09 and 13.2 ± 4.067 cells in the Sham-exposed and Naïve rat groups).

SMF exposure of early postnatal rat primary cortical neuronal cultures stimulates a pro-neurogenic response

The increase in newly generated DCX^+/EdU^+ cells was also evident in cultured rat primary cortical neurons exposed to weak SMF (5 mT) over a 7-day course

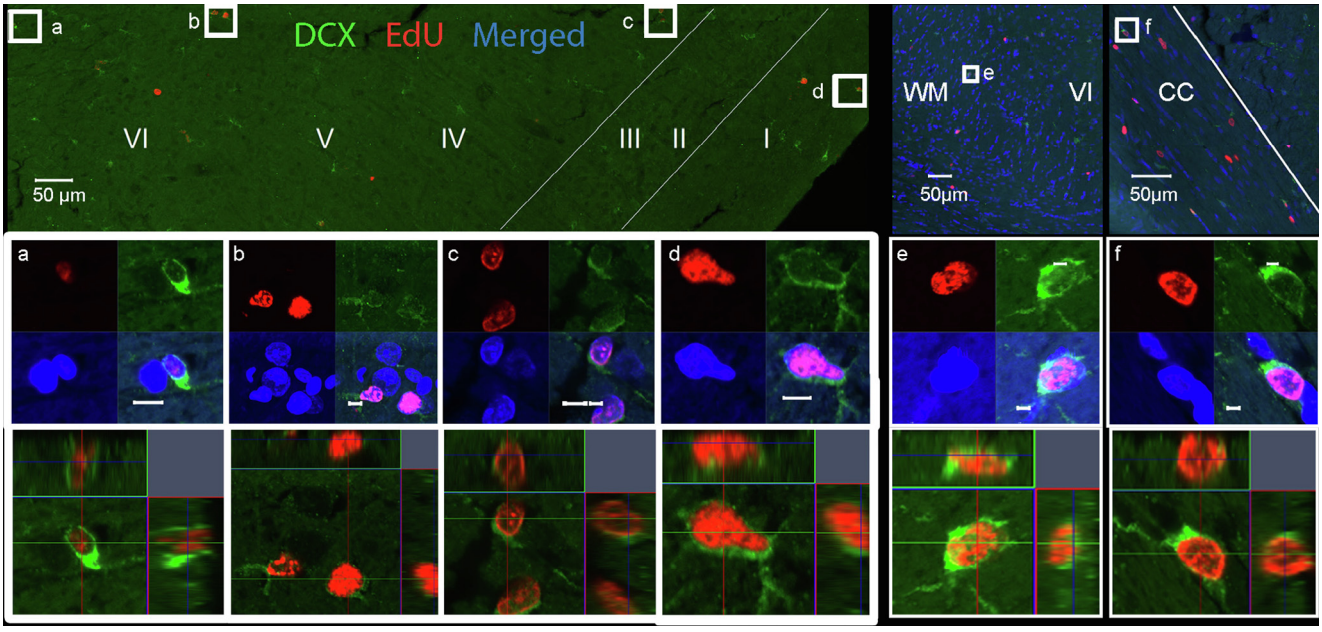

Fig. 4. This figure demonstrates the occurrence of DCX^+/EdU^+ cells across cortical layers I–VI (**a–d**), the WM and CC (**e, f**). Magnified images are accompanied by the orthogonal projections from a 12 consecutive *z*-axis image stack (1.16 μm). Scale bars in magnifications (middle row) indicate 5 μm.

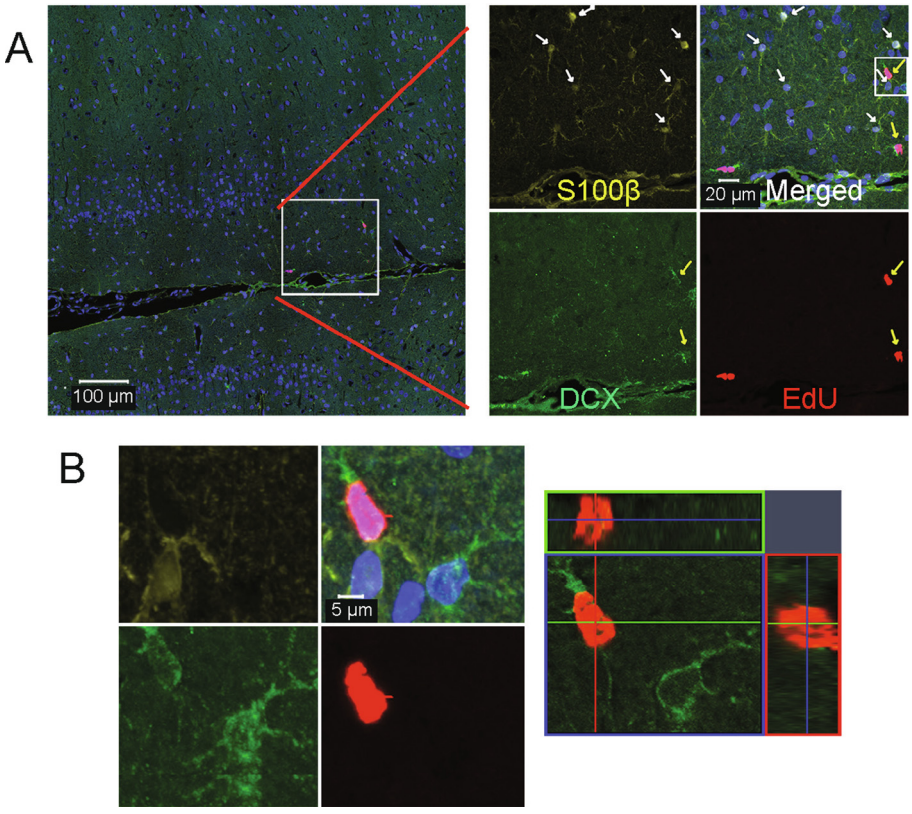

Fig. 5. DCX$^+$/EdU$^+$ cells in the neocortex do not co-express the glial marker S100ß. (**A**) Confocal images of a representative neocortical brain section (bregma: −1.88 mm) co-stained with antibodies against DCX, EdU, and S100ß, showing the distribution of DCX, EdU, S100ß- (white arrows) and DCX/EdU- (yellow arrows) labeled cells. Nuclear staining with Hoechst-33342. (**B**) Confocal and orthogonal magnification images of DCX$^+$/EdU$^+$ cell show negative staining for S100ß. (For interpretation of the references to colour in this figure legend, the reader is referred to the web version of this article.)

(Fig. 6). SMF and control cultures had similar proportions of DCX$^+$ cells, typical of the early postnatal period [48.39%, Interquartile Range (IQR) = 13.34, and 55.12%, IQR = 24.34, respectively, representing the median cell percentage and IQR for $n = 4$ in each group, $p > 0.05$, $U(4,4) = 6.0$, Fig. 6B]. However, the proportion of DCX$^+$ cells that were newly generated was 2.3-fold higher in SMF-exposed cultures, compared with the corresponding cell population in control cultures co-labeled with DCX and EdU. While 1.8 ± 0.21% of the cells were co-labeled with DCX and EdU in the control cultures, 4.1 ± 0.54% of DCX$^+$ cells in SMF-exposed cultures co-expressed EdU [mean cell percentage ± SEM is presented for $n = 4$ in each group, $p < 0.01$, $t(6) = 4.024$, Fig. 6C]. Further labeling cells with late phase neuronal marker NeuN to detect mature neurons, we detected mature neurons that had incorporated proliferation markers (either BrdU or EdU) into their nuclei (Fig. 6F). Upon quantification, we found more than a 2-fold increase in the fraction of mature neurons recently generated in SMF-exposed cultures, compared with control [5.4 ± 0.76% of the NeuN$^+$ neurons co-labeled with EdU, compared with 2.1 ± 0.83% of the neurons in control cultures; mean cell percentage ± SEM for $n = 4$ in each group, $p < 0.05$, $t(6) = 2.96$ Fig. 6F]. This indicates a stimulation of early postnatal neurogenesis by SMF exposure.

To explore whether SMF exposure also activates genes that may direct cells into neuronal lineage, we analyzed the mRNA expression profile of neurogenesis–related genes in primary cortical neurons. We found that a short exposure of the neurons to SMF (5 mT, 72 h) activates pro-neuronal bHLH transcription factors that drive postnatal neuronal fate commitment and support neurogenesis (Ross et al., 2003). As depicted in Fig. 6G, cortical neurons exposed to SMF activated different classes of bHLH genes, increasing the mRNA expression of the Achaete-Scute homolog 1 Mash1, a broadly expressed pro-neural transcription factor, to 1. 9 ± 0.13 fold of control, [$p < 0.001$, $t(10.51) = 5.994$, $n = 11$], as well as NeuroD1 [to 2.2 fold of control (median values), IQR = 4.2, $U(10,10) = 1.0$, $p < 0.0001$] and NeuroD2 [to 5.0 ± 1.12 fold of control (mean +/− SEM), $p < 0.01$, $t(12.02) = 3.58$, $n = 13$], neuronal subtype specific transcription factors expressed post-mitotically (Bertrand et al., 2002). SMF exposure also increased the expression of the Atonal Atoh-1 [2. 8 ± 0.42 fold of control, $p < 0.01$, $t(10.41) = 4.06$, $n = 11$], Neurogenin-1 [1.8 fold of control, IQR = 4.69, median ± IQR values are given, $U(13,13) = 20.0$, $p < 0.001$] and Neurogenin-2 [2.0 ± 0.18 fold of control, $p < 0.01$, $t(6.225) = 5.25$, $n = 6$] (Fig. 6G), expressed in early mitotic precursor cells. Altogether, our data point to a pro-neurogenic effect of SMF exposure, which stimulates early and late phases of neuronal differentiation while activating pro-neurogenic genes.

DISCUSSION

In this study, we show that a 3-week continuous exposure of young adult rats to low intensity (< 10 mT) SMF significantly increases the population of DCX$^+$/EdU$^+$ cells in the SVZ and neocortex. Modulators of SVZ neurogenesis in the adult brain are of major scientific interest due to the therapeutic potential of neuronal precursors constitutively produced in the SVZ during adulthood, generating a reservoir of neuroblasts that may be harnessed to brain repair purposes. SVZ neuroblasts are generated *in situ* and migrate in chain-like structures through the rostral migratory stream

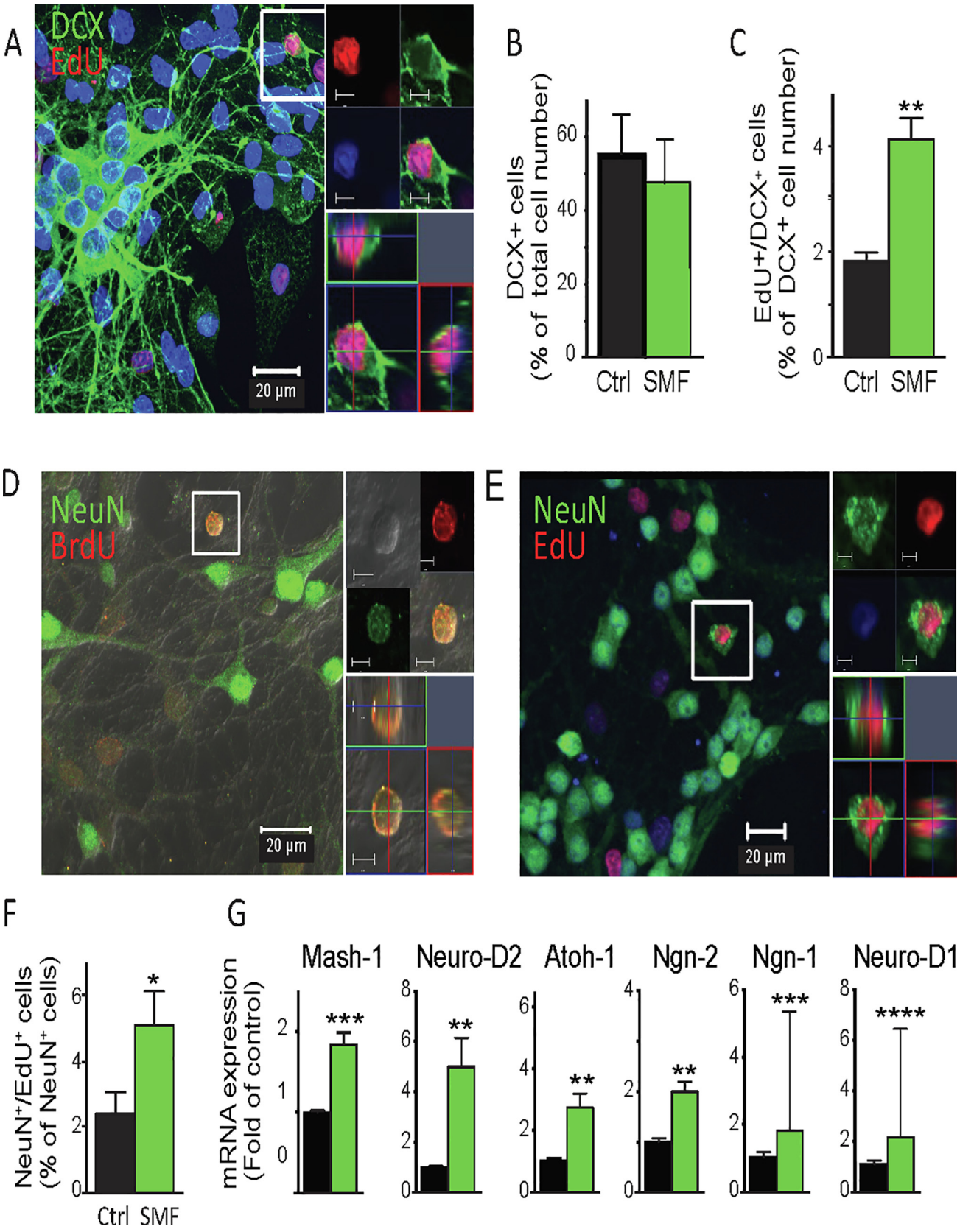
A
DCX
EdU
20 μm
B
DCX+ cells
(% of total cell number)
60
40
20
0
Ctrl SMF
C
EdU+/DCX+ cells
(% of DCX+ cell number)
**
4
2
0
Ctrl SMF
D
NeuN
BrdU
20 μm
E
NeuN
EdU
20 μm
F
NeuN+/EdU+ cells
(% of NeuN+ cells)
*
6
4
2
0
Ctrl SMF
G
mRNA expression
(Fold of control)
Mash-1
***
Neuro-D2
**
Atoh-1
**
Ngn-2
**
Ngn-1
***
Neuro-D1
****

(RMS) towards the olfactory bulb (OB), where they complete their differentiation into local granule or periglomerular interneurons that ultimately integrate into the local synaptic network. However, studies show that these neuroblasts do attain a principle capability to emigrate from the SVZ in routes other than the RMS-OB axis, a property that may have particular importance in conditions such as brain injury. For instance, in response to damage, SVZ neuroblasts disperse from the RMS as individual cells, and emigrate out of the SVZ towards adjacent lesioned sites, as shown in the post stroke adult striatum (Yamashita et al., 2006) and cortex (Sundholm-Peters et al., 2005; Jin et al., 2003). SVZ neuroblast migration to the cortex was also demonstrated following cortical aspiration lesion and neocortical apoptosis induction (Saha et al., 2013; Magavi et al., 2000).

At the lesion site, SVZ neuroblasts either support the maintenance of pre-existing neurons by the release of neurotrophic factors or endocannabinoids that protect against toxicity (Sabelstrom et al., 2013; Butti et al., 2012), or differentiate into mature neurons and therefore provide a potential regenerative support (Yamashita et al., 2006). However, the small fraction of SVZ neuroblasts that actually reaches the injured site and replaces merely a small proportion of the damaged neurons was claimed insufficient to induce a substantial neurological improvement (Arvidsson et al., 2002). Nevertheless, although this reaction is limited, it alludes to a latent regenerative potential of precursors residing in the SVZ in the adult brain that may be activated following specific cues, and potentially contribute to brain repair following injury or neurodegenerative diseases.

In addition to the enhancement of SVZ DCX^+/EdU^+ neuroblast generation by SMF exposure, our results also indicate a constitutive generation of DCX^+ cells in the neocortex of young adult rats, which is further enhanced by SMF exposure. Our findings are in line with other studies demonstrating the sensitivity of cortical PSA-$NCAM^+$ or DCX^+ cells to environmental stimuli (Xiong et al., 2010) and pharmacological manipulations (Guirado et al., 2012; Frasca et al., 2008). The cytoskeleton-associated protein DCX is transiently expressed by migrating neuroblasts during development (Francis et al., 1999; Gleeson et al., 1999). In the adult brain, DCX is predominantly expressed by migrating type A SVZ neuroblasts (Brown et al., 2003) and hippocampal DG progenitor cells during neuronal commitment stages, reflecting the neurogenic activity in these regions.

In recent decades, it has become evident that DCX expression in the adult brain extends beyond these canonical niches, as indicated by the detection of DCX^+ cells in the striatum, corpus callosum (CC) and layers II/III of the paleocortex, in particular the piriform and lateral entorhinal cortices in rodents (Klempin et al., 2011; Shapiro et al., 2007; Pekcec et al., 2006; Nacher at al., 2001; Seki and Arai, 1991). DCX^+ cells were also detected in layer II of the neocortex in higher mammals such as rabbits, guinea pigs and primates (Yang et al., 2015; Bonfanti and Nacher, 2012; Bloch et al., 2011; Luzzati et al., 2009; Gomez-Climent et al., 2008; Xiong et al., 2008). However, the pre- (Yang et al., 2015; Gomez-Climent et al., 2008; Shapiro et al., 2007) or post-natal (Xiong et al, 2010; Pekcec et al., 2006) origin of these cells, as well as the interpretation of DCX expression in adulthood outside the canonical neurogenic niches with respect to early stages of ongoing neurogenesis, are controversial. DCX may be up-regulated in pre-existing neurons in a manner which is uncoupled from adult neurogenesis, for instance, in processes such as microtubule reorganization and stabilization that require the involvement of DCX (Moores et al., 2004). Moreover, DCX^+ cells detected in the piriform cortex, previously linked to neurogenesis in this region, were later classified as a unique class of pre-existing immature neurons generated over the prenatal phases of corticogenesis, that maintain a prolonged immature state (Gomez-Climent et al., 2008), or as pre-existing neurons undergoing structural plasticity (Bonfanti and Nacher, 2012). The generation of new neurons in the adult neocortex was documented in response to damage in several studies (Tsai et al., 2006; Chen et al., 2004; Magavi et al., 2000; Arvidsson et al., 2002), while others have either failed to detect adult neurogenesis in this region (Huttner et al., 2014; Bhardwaj et al., 2006; Ehninger and Kempermann, 2003; Koketsu et al., 2003; Kornack and Rakic, 2001), or demonstrated a low level of neurogenesis which persists under physiological conditions in the neocortex of adult monkeys (Bernier et al., 2002; Gould et al., 2001; Gould et al, 1999), rabbits (Ponti et al., 2008; Luzzati et al., 2006) and rodents (Dayer al., 2005; Kaplan, 1981), generated from either cortical progenitor cells (Dayer et al., 2005; Magavi

Fig. 6. SMF-exposure stimulates a pro-neurogenic response in rat primary cortical neurons. Primary cortical neurons were exposed to 5 mT SMF for 7 days, treated with EdU (10 μM) or BrdU (10 μM) on DIV2 and DIV6 and co-stained for neuronal and proliferation markers, BrdU/NeuN, EdU/NeuN. Nuclei were observed using 33342-Hoechst. (**A**) Confocal z-stack image of 12 consecutive 1.16 μm images and orthogonal projection of a cell co-expressing DCX/EdU (scale bar in magnification indicates 5 μm). (**B**) Quantification of the number of DCX+ cells relative to the total cell number, in SMF and control cultures ($p > 0.05$, $n = 4$). (**C**) Comparison of DCX^+/EdU^+ cell fraction in SMF-exposed and control cultures, showing a higher percentage of DCX^+/EdU^+ cells in SMF-exposed cultures (**$p < 0.01$, $n = 4$). (**D, E**) Mature $NeuN^+$ neurons exposed to SMF express the proliferation markers BrdU (**D**) and EdU (**E**), scale bars in high-magnification images indicate 5 μm. (**F**) Quantification of $NeuN^+/EdU^+$ co-localization shows a higher percentage of NeuN/EdU co-localization in SMF-exposed neuronal cultures (**$p < 0.05$, $n = 4$). The results of a representative experiment are shown in (**B**), (**C**) and (**F**). All results were replicated in at least 3 independent experiments. (**G**) The effect of 72 h (DIV5-DIV7) SMF exposure on gene expression in primary cortical cultures. The fold increase in mRNA expression of bHLH genes compared with control, determined by the ddCT method and normalized to the level of a house-keeping gene is presented for each gene. All results were replicated in at least 3 independent experiments. Data in **C** and **F** were analyzed using two-tail Student's *t*-test (Mean values ± SEM are presented), and data in **B** were analyzed using Mann-Whitney test (Median and IQR values are shown). Data in **G** were analyzed in either two-tailed *t*-test with Welch's correction for unequal variances [Mash1(***$p < 0.001$), NeuroD2 (**$p < 0.01$), Atoh-1 (**$p < 0.01$), Ngn-2 (**$p < 0.01$), mean ± SEM of at least 3 experiments are shown], or non-parametric Mann-Whitney test [NeuroD1 (****$p < 0.0001$) and Ngn-1 (***$p < 0.001$), median and IQR values are shown].

et al., 2000) or SVZ neuroblasts (Inta et al., 2008; Gould et al., 1999).

In order to maximize the number of proliferating cells labeled by EdU across the entire study period (21 days), and given the limited availability of thymidine analogs for labeling post injection (Hayes and Nowakowski, 2000), we used a multiple EdU injection regime. Using a high magnification confocal microscope (equipped with a X40 objective), we were able to detect a low level of DCX^+/EdU^+ cells sparsely distributed throughout all neocortical layers of young adult rats from all experimental groups, including Naïve rats, supporting the notion of a spontaneous constitutive generation or migration of these cells during the postnatal period. SMF exposure doubled the number of these cells, enhancing their detectability. Unlike previous findings from studies in higher mammals, DCX^+/EdU^+ cells detected in the rats' neocortex were not organized in a particular pattern, but rather randomly scattered as either individual cells or cell doublets. Additionally, DCX^+ cells analyzed in this study incorporated EdU into healthy, non-apoptotic integrated nuclei, as reflected by nuclear 33342-Hoechst staining, implying that these cells were not synthesizing DNA while dying, thus excluding a possibility of DNA repair as the cause for s-phase EdU incorporation. The number of EdU^+-, DCX^+-, or DCX^+/EdU^+ in the SVZ or neocortex of Naïve rats did not differ from the corresponding cell numbers in the operated (Sham control) group, indicating that the surgical procedure had no effect on cell proliferation or DCX^+ expression at the time of measurement (3 weeks post-surgery). In the findings described herein, SMF exposure increased the number of DCX^+/EdU^+ and EdU^+ cells in the SVZ, and DCX^+/EdU^+ cells in the neocortex without affecting the total number of DCX^+ cells. DCX expression by immature neurons is down-regulated within 15–21 days (Brown et al., 2003). If some immature neurons were generated earlier on during the 21-day experimental course, it is possible that by the end of the experiment, these DCX expressing cells had already down-regulated their DCX expression and therefore appeared as a DCX^-/EdU^+ cell at the experiment's end point. Moreover, we have previously shown that SMF exposure affects glial cell apoptosis in addition to that of neurons (Ben Yakir-Blumkin et al., 2014). Therefore, it cannot be excluded that the effect of SMF on cell proliferation *in vivo* is more general and affects additional cell populations, such as glial, oligodendrocytes (Prasad et al., 2017) and other precursor cells residing in the examined brain regions, or that in proliferating cells labeled in the last injection before animals were sacrificed, DCX was still undetectable. Such a scenario may explain the similar abundance of DCX^+ cells despite the increase in DCX^+/EdU^+ cells.

The SVZ is a main source of proliferative neuronal progenitor cells during development as well as in adulthood (Urban and Guillemot, 2014). As discussed earlier, SVZ neuroblasts attain the ability to migrate from the SVZ towards the adjacent striatum and neocortex following lesion (Yang and Levison, 2007; Yamashita et al., 2006; Sundholm-Peters et al., 2005; Jin et al., 2003; Magavi et al., 2000). An early postnatal migration of SVZ precursors towards cortical and subcortical structures was also demonstrated in transgenic mice expressing EGFP in 5-HT3-positive neurons (Inta et al., 2008), and SVZ neuroblasts migrate through the CC to the frontal neocortical regions in adult macaque monkeys (Gould et al., 1999). The morphological resemblance between the newly generated neocortical cells described in this study and migrating SVZ neuroblasts, along with their detection in deep cortical layers, WM and CC, regions positioned in close proximity to the SVZ, may allude to a possible origin of some of these cells in the SVZ. Moreover, some of the newly generated neocortical cells described in this study were detected as cell doublets (for example, see Fig. 3 Bk), or positioned closely (2–3 μm) to another DCX^+/EdU^+ cell. This may indicate the *in situ* generation of DCX^+/EdU^+ cells from local precursors, known to reside in different regions of the adult brain. The cortex contains latent progenitor cells that can be activated when exposed to specific cues such as growth factors (Homman-Ludiye et al., 2012; Palmer et al., 1999) or lesion. For instance, quiescent progenitors residing in layer I of the rat cerebral cortex are activated after ischemia, giving rise to new cortical interneurons (Ohira et al., 2010). DCX-expressing Oligodendroglial Progenitor Cells (OPCs) residing in the adult murine piriform cortex were shown to differentiate into pyramidal glutamatergic neurons (Guo et al., 2010). Postnatal OPCs were reported as multipotent cells that may differentiate into astrocytes and neurons in multiple regions of the adult CNS (Guo et al., 2009, Rivers et al., 2008, Tamura et al., 2007), although the neuronal lineage of these cells is debatable (Nishiyama et al., 2016; Kang et al., 2010).

The origin as well as fate of DCX^+/EdU^+ neocortical cells described in this study warrants further investigation, but taken together, our findings show that SMF exposure stimulates the generation, or migration, of new neocortical cells with neuronal lineage potential. Our findings showing that 5.5–7.7% of the EdU^+ cells in the neocortex express NeuN within 14 days after EdU injection do align with the previously described time course for NeuN expression post multiple BrdU injections in rats (Brown et al., 2003). The low incidence of $EdU^+/NeuN^+$ in the neocortex described in this study may indicate that a duration of more than 14 days post-labeling is required for detection of mature neuronal phenotype. However, the notion of a pro-neurogenic stimulatory effect of SMF exposure is supported by our *in vitro* findings, showing that SMF exposure increases both the fraction of DCX^+/EdU^+ cells and NeuN-expressing neurons co-labeled with EdU, while activating pro-neural bHLH genes that support neurogenesis.

The bHLH genes encode transcription factors that regulate cell fate decision both in embryonic development and in the adult brain (Zhang and Jiao, 2015). In adulthood, these factors are expressed by the neurogenic niches and direct neuronal commitment via activation of different sub-groups of pro-neuronal activator-type genes such as Atonal (*Math1*), Achaete-Scute (*Mash1*), Neurogenin (*Ngn1*, *Ngn2*) and NeuroD families (*NeuroD1, NeuroD2*) (Kim et al., 2011; Boutin

et al., 2010; Sun et al., 2001), while suppressing neurogenesis by repressor-type genes that regulate neuronal precursor self renewal, maintaining cells in an undifferentiated state (Bai et al., 2007). Alterations in activator bHLH genes were previously demonstrated in response to ELFMF as well as radio frequency MF exposure (Chen et al., 2014; Ma et al., 2014; Leone et al., 2014). For example, an up-regulation of NeuroD1 and Ngn1 was observed in differentiating embryonic (E13.5) neuronal stem cells (eNSCs) intermittently exposed to 50 Hz ELFMF (1 mT) (Ma et al., 2016). In the adult brain, increased expression of Mash1, NeuroD2 and Hes1 genes was associated with enhanced hippocampal DG neurogenesis observed in C57BL/6 mice exposed to 50 Hz ELFMF (1mT) (Cuccurazzu et al, 2010).

In this study, SMF exposure activated the pro-neuronal *Ascl1, Neurog1* and *Neurog2,* transcription factors that support neurogenesis by promoting differentiation and neuronal cell fate (Boutin et al., 2010; Sun et al., 2001; Bertrand et al, 2002; Bai et al., 2007). *Neurod1,* also activated by SMF exposure, is expressed late during CNS developmental phase, and was found to be essential for differentiation and survival of neurons generated in adulthood (Gao et al., 2009). The activation of bHLH genes indicates that SMF exposure may support the direction of newly generated neocortical cells towards a neuronal lineage. The transcription of genes that regulate cell survival and differentiation, such as bHLH genes, is modulated by Ca^{2+} influx through L-type VGCCs (West et al., 2001; Hardingham et al., 1998). For instance, the activation of L-type VGCCs in adult rat hippocampal model of progenitor cells was shown to inhibit the expression of genes involved in glial cell fate and enhance the expression of NeuroD (Deisseroth et al., 2004). Other studies have shown that the phosphorylation and activation of NeuroD1 and NeuroD2 is triggered by Ca^{2+} influx into precursor cells (Ince-Dunn et al., 2006; Olson et al., 2001). We have previously shown that the pro-survival activity of SMF exposure (5 mT) in primary cortical neurons is mediated by Ca^{2+} influx through L-type VGCCs (Ben Yakir-Blumkin et al., 2014). It is therefore possible that the pro-neurogenic effect of low intensity SMF exposure described in this paper, which involves bHLH gene activation, is related to an upstream VGCCs activation and Ca^{2+} influx modulation, previously observed in response to SMF exposure. Increased hippocampal neurogenesis in mice *in vivo* by 50 Hz, 1mT ELFMF (Cuccurazzu et al., 2010) is also accompanied by activation of the bHLH gene group, as was the increased neocortical and hippocampal progenitor cell formation in neurospheres prepared from E18 rat embryos exposed to 100 mT SMF (Nakamichi et al., 2009). Recently, ELFMF exposure of mice was shown to enhance SVZ neurogenesis which is dependent on the Wnt pathway (Mastrodonato et al., 2018).

In this study, we show for the first time that a population of new DCX^+/EdU^+ cells in the SVZ and neocortex is responsive to SMF exposure, which enhanced the generation of both SVZ neuroblasts and new neocortical cells with neuronal lineage potential in the adult rat brain. Our *in vitro* findings support the pro-neurogenic effect of SMF-exposure observed *in vivo*.

Stimulation of neurogenesis in the adult brain may compensate for neuronal loss occurring in traumatic brain injury and pathological conditions such as neurodegenerative diseases, where adult SVZ neurogenesis is perturbed and massive neuronal populations in distinct brain regions, including the neocortex, are lost. SMFs, previously shown to reduce cortical apoptotic cell death that underlies AD, may offer new avenues for brain repair.

Mathematical derivation of magnetic field strengths at known distance from a permanent cylindrical magnet

Our purpose in the framework of this derivation is to establish the magnetic field distribution of azimuthally symmetric permanent magnet of radius R and height h. Since the magnetic induction $B[\mathrm{V}\cdot\mathrm{sec}\cdot\mathrm{m}^{-2}]$ is defined in terms of the magnetic field $H[\mathrm{A}\cdot\mathrm{m}^{-1}]$, the vacuum permeability coefficient $\mu_0\left(=4\pi\times10^{-7}\right)$ and the magnetization field $M[\mathrm{A/m}]$ by $\vec{B}=\mu_0\left(\vec{H}+\vec{M}\right)$ and keeping in mind that $\vec{\nabla}\cdot\vec{B}=0$ we have

$$\vec{\nabla}\cdot\vec{H}=-\vec{\nabla}\cdot\vec{M} \tag{1}$$

wherein the divergence operator on an arbitrary vector is defined by $\vec{\nabla}\cdot\vec{A}=\frac{1}{r}\frac{\partial rA_r}{\partial r}+\frac{1}{r}\frac{\partial A_\phi}{\partial\phi}+\frac{\partial A_z}{\partial z}$, the vector function in cylindrical coordinates (r,ϕ,z), $\vec{M}(r,z)=M_0\vec{1}_z\left[u\left(z+\frac{1}{2}h\right)-u\left(z-\frac{1}{2}h\right)\right]u(R-r)$, is an approximation of the magnetization inside a permanent magnet. For our specific case, the diameter is $2R=3$mm whereas the thickness $h=0.7$mm, M_0 is the intrinsic magnetization of the magnet and $u(z)$ is the Heaviside step function and it is explicitly given by $u(z<0)=0$ and $u(z>0)=1$. Introducing, the gradient and the magnetic scalar potential ψ namely, $\vec{H}=\nabla\psi\equiv\frac{\partial\psi}{\partial r}\hat{n}_r+\frac{1}{r}\frac{\partial\psi}{\partial\phi}\hat{n}_\phi+\frac{\partial\psi}{\partial z}\hat{n}_z$ with $\vec{n}\left(=\hat{n}_r+\hat{n}_\phi+\hat{n}_z\right)$ representing the unit vector in cylindrical coordinates, we get the Poisson equation with the magnetization as the source term

$$\nabla^2\psi\equiv\frac{1}{r}\frac{\partial}{\partial r}r\frac{\partial\psi}{\partial r}+\frac{1}{r^2}\frac{\partial^2\psi}{\partial\phi^2}+\frac{\partial^2\psi}{\partial z^2}=-\vec{\nabla}\cdot\vec{M} \tag{2}$$

and in the absence of ferromagnetic or permeable materials we can assume that the distribution of the magnetic field is identical to that of free space thus with the latter's Green's function we get

$$\psi\left(\vec{r}\right)=\int d\vec{r}'\frac{\vec{\nabla}\cdot\vec{M}}{4\pi\left|\vec{r}-\vec{r}'\right|} \tag{3}$$

Substituting the explicit expression for the magnetization

$$\psi\left(\vec{r}\right)=\frac{M_0}{4\pi}\int dx'dy'\left\{\frac{u(R-r')}{\sqrt{(x-x')^2+(y-y')^2+\left(z+\frac{1}{2}h\right)^2}}-\frac{u(R-r')}{\sqrt{(x-x')^2+(y-y')^2+\left(z-\frac{1}{2}h\right)^2}}\right\} \tag{4}$$

wherein $\delta(z)$ is Dirac's delta function; note that the center of the cylindrical magnet coincides with the zero of the

coordinate system. Employing cylindrical co-ordinates we get

$$\psi(r,\phi,z)=\frac{M_0}{4\pi}\int_0^R dr'r'\int_0^{2\pi}d\phi'\left\{\begin{array}{l}\frac{1}{\sqrt{r^2+r'^2+\left(z+\frac{1}{2}h\right)^2-2rr'\cos\left(\phi'-\phi\right)}}\\-\frac{1}{\sqrt{r^2+r'^2+\left(z-\frac{1}{2}h\right)^2-2rr'\cos\left(\phi'-\phi\right)}}\end{array}\right\} \tag{5}$$

and further we define

$$U(a)\equiv\frac{1}{2\pi}\int_0^{2\pi}d\phi\frac{1}{\sqrt{1-a\cos\phi}}\simeq 1+\frac{3}{16}a^2+O(a^4) \tag{6}$$

enabling

$$\psi(r,z)=\frac{M_0}{2}\int_0^R dr'r'\left\{\begin{array}{l}\frac{1}{\sqrt{r^2+r'^2+\left(z+\frac{1}{2}h\right)^2}}U\left(\frac{2rr'}{r^2+r'^2+\left(z+\frac{1}{2}h\right)^2}\right)\\-\frac{1}{\sqrt{r^2+r'^2+\left(z-\frac{1}{2}h\right)^2}}U\left(\frac{2rr'}{r^2+r'^2+\left(z-\frac{1}{2}h\right)^2}\right)\end{array}\right\} \tag{7}$$

We aim to determine the intensity of the total magnetic induction namely:

$$B(r,z)\equiv\sqrt{B_r^2(r,z)+B_z^2(r,z)}=\mu_0\sqrt{\left(\frac{\partial\psi}{\partial r}\right)^2+\left(\frac{\partial\psi}{\partial z}\right)^2} \tag{8}$$

So far we have tacitly assumed that the intrinsic magnetic field is known. While in practice this is provided by the supplier, we preferred our own assessment by calculating the magnetic induction along the z-axis. Assuming the probe of the Gaussmeter has zero thickness the measured magnetic field B at ζ distance from the source is:

ζ[mm]	$B_{\exp}[G]$
0	700
1	350
2	130
3	75
4	41
5	28
6	14
7	10
8	8
9	5
10	4

(9)

It can be shown both theoretically as well as experimentally that at $r=0$ the far field satisfies

$$B(0,\zeta)\zeta^3\sim\text{const.} \tag{10}$$

The distances are measured in millimeters and the coefficient B_0 is determined by minimizing the Error from the experimental and theoretical approximation

$$\text{Error}(B_0)=100\frac{\sum_{i=0}^{10}\left\{\zeta_i^3\left[B_{\exp,i}-B_0\bar{B}\left(r=0,\zeta_i\right)\right]\right\}^2}{\sum_{i=0}^{10}\left\{\zeta_i^3B_{\exp,i}\right\}^2} \tag{11}$$

wherein $B_0=\mu_0M_0$ and $\bar{B}\left(r,z\right)\equiv B(r,z)/B_0$ thus

$$\frac{d}{dB_0}\text{Error}(B_0)=0\ \Rightarrow\ B_0=\frac{\sum_{i=0}^{10}\zeta_i^6B_{\exp,i}\bar{B}\left(r=0,\zeta_i\right)}{\sum_{i=0}^{10}\zeta_i^6\bar{B}^2(r=0,\zeta_i)} \tag{12}$$

Subject to the assumption that the probe is of negligible thickness $(d=0)$ the error is 2.4% and B_0 4.6×10^3 [G].

Next we determine the impact of the *thickness* of the Gaussmeter's probe by assuming that $\zeta_{d,i}=\zeta_i+d$. We repeat the procedure based upon

$$\text{Error}(B_0,d)=100\frac{\sum_{i=0}^{10}\left\{\zeta_{d,i}^3\left[B_{\exp,i}-B_0\bar{B}\left(r=0,\zeta_{d,i}\right)\right]\right\}^2}{\sum_{i=0}^{10}\left\{\zeta_{d,i}^3B_{\exp,i}\right\}^2} \tag{13}$$

which has a minimum for $B_0\sim7.1\times10^3$ [G] and $d\sim1$ mm corresponding to an error of 0.8%.

ACKNOWLEDGEMENTS

The authors thank Edith Suss-Toby and the Technion's Bio Core Facility Microscopy Unit devoted staff members for assistance with confocal data acquisition and analysis, Yotam Shem-Tov for constructive comments and assistance with statistical analyses, and Naama Klopstock for technical support with real time PCR preparations.

COMPLIANCE WITH ETHICAL STANDARDS

Conflict of interest: The authors declare that they have no conflict of interest.

Animal experimentation: All procedures with animals were authorized by the Technion's Animal Care and Use Committee, whose ethical standards are based on those detailed in the National Institutes of Health (Bethesda, MD) Guide for the Care and Use of Laboratory Animals, and whose general procedures for animal welfare comply with Israeli law on animal experimentation.

REFERENCES

Alvarez-Buylla A, Garcia-Verdugo JM (2002) Neurogenesis in adult subventricular zone. J Neurosci 22:629–634.

Arias-Carrion O, Verdugo-Diaz L, Feria-Velasco A, Millan-Aldaco D, Gutierrez AA, Hernandez-Cruz A, et al. (2004) Neurogenesis in the subventricular zone following transcranial magnetic field stimulation and nigrostriatal lesions. J Neurosci Res 78:16–28.

Arvidsson A, Collin T, Kirik D, Kokaia Z, Lindvall O (2002) Neuronal replacement from endogenous precursors in the adult brain after stroke. Nat Med 8:963–970.

Bai G, Sheng N, Xie Z, Bian W, Yokota Y, Benezra R, et al. (2007) Id sustains Hes1 expression to inhibit precocious neurogenesis by releasing negative autoregulation of Hes1. Dev Cell 13:283–297.

Ben Yakir-Blumkin M, Loboda Y, Schachter L, Finberg JP (2014) Neuroprotective effect of weak static magnetic fields in primary neuronal cultures. Neuroscience 278:313–326.

Bernier PJ, Bedard A, Vinet J, Levesque M, Parent A (2002) Newly generated neurons in the amygdala and adjoining cortex of adult primates. Proc Natl Acad Sci USA 99:11464–11469.

Bertrand N, Castro DS, Guillemot F (2002) Proneural genes and the specification of neural cell types. Nat Rev Neurosci 3:517–530.

Bhardwaj RD, Curtis MA, Spalding KL, Buchholz BA, Fink D, Bjork-Eriksson T, et al. (2006) Neocortical neurogenesis in humans is restricted to development. Proc Natl Acad Sci USA 103 (33):12564–12568.
Bloch J, Kaeser M, Sadeghi Y, Rouiller EM, Redmond Jr DE, Brunet JF (2011) Doublecortin-positive cells in the adult primate cerebral cortex and possible role in brain plasticity and development. J Comp Neurol 519:775–789.
Bonfanti L, Nacher J (2012) New scenarios for neuronal structural plasticity in non-neurogenic brain parenchyma: the case of cortical layer II immature neurons. Prog Neurobiol 98:1–15.
Brown JP, Couillard-Despres S, Cooper-Kuhn CM, Winkler J, Aigner L, Kuhn HG (2003) Transient expression of doublecortin during adult neurogenesis. J Comp Neurol 467:1–10.
Bonfanti L, Olive S, Poulain DA, Theodosis DT (1992) Mapping of the distribution of polysialylated neural cell adhesion molecule throughout the central nervous system of the adult rat: an immunohistochemical study. Neuroscience 49:419–436.
Boutin C, Hardt O, de Chevigny A, Core N, Goebbels S, Seidenfaden R, et al. (2010) NeuroD1 induces terminal neuronal differentiation in olfactory neurogenesis. Proc Natl Acad Sci USA 107:1201–1206.
Buck SB, Bradford J, Gee KR, Agnew BJ, Clarke ST, Salic A (2008) Detection of S-phase cell cycle progression using 5-ethynyl-2'-deoxyuridine incorporation with click chemistry, an alternative to using 5-bromo-2'-deoxyuridine antibodies. Biotechniques 44:927–929.
Butti E, Bacigaluppi M, Rossi S, Cambiaghi M, Bari M, Cebrian Silla A, et al. (2012) Subventricular zone neural progenitors protect striatal neurons from glutamatergic excitotoxicity. Brain 135(Pt 11):3320–3335.
Carter R, Aspy CB, Mold J (2002) The effectiveness of magnet therapy for treatment of wrist pain attributed to carpal tunnel syndrome. J Fam Practice 51:38–40.
Chen C, Ma Q, Liu C, Deng P, Zhu G, Zhang L, et al. (2014) Exposure to 1800 MHz radiofrequency radiation impairs neurite outgrowth of embryonic neural stem cells. Sci Rep-UK 4:5103.
Chen J, Magavi SS, Macklis JD (2004) Neurogenesis of corticospinal motor neurons extending spinal projections in adult mice. Proc Natl Acad Sci USA 101:16357–16362.
Cuccurazzu B, Leone L, Podda MV, Piacentini R, Riccardi E, Ripoli C, et al. (2010) Exposure to extremely low-frequency (50 Hz) electromagnetic fields enhances adult hippocampal neurogenesis in C57BL/6 mice. Exp Neurol 226:173–182.
Dash PK, Mach SA, Moore AN (2001) Enhanced neurogenesis in the rodent hippocampus following traumatic brain injury. J Neurosci Res 63:313–319.
Dayer AG, Cleaver KM, Abouantoun T, Cameron HA (2005) New GABAergic interneurons in the adult neocortex and striatum are generated from different precursors. J Cell Biol 168:415–427.
Deisseroth K, Singla S, Toda H, Monje M, Palmer TD, Malenka RC (2004) Excitation-neurogenesis coupling in adult neural stem/progenitor cells. Neuron 42:535–552.
Duman RS (2004) Depression: a case of neuronal life and death? Biol Psychiat 56:140–145.
Ehninger D, Kempermann G (2003) Regional effects of wheel running and environmental enrichment on cell genesis and microglia proliferation in the adult murine neocortex. Cereb Cortex 13:845–851.
Eichholz GG (2002) Non-ionizing radiation, part 1: static and extremely low-frequency (ELF) electric and magnetic fields, IARC monographs on the evaluation of carcinogenic risk to humans. Health Phys 83:920.
Eriksson PS, Perfilieva E, Bjork-Eriksson T, Alborn AM, Nordborg C, Peterson DA, et al. (1998) Neurogenesis in the adult human hippocampus. Nat Med 4:1313–1317.
Eriksson PS (2006) Schizophrenia – a stem cell disorder. Exp Neurol 199:26–27.
Francis F, Koulakoff A, Boucher D, Chafey P, Schaar B, Vinet MC, et al. (1999) Doublecortin is a developmentally regulated, microtubule-associated protein expressed in migrating and differentiating neurons. Neuron 23:247–256.
Frasca A, Fumagalli F, Ter Horst J, Racagni G, Murphy KJ, Riva MA (2008) Olanzapine, but not haloperidol, enhances PSA-NCAM immunoreactivity in rat prefrontal cortex. Int J Neuropsychop 11:591–595.
Gage FH (2000) Mammalian neural stem cells. Science 287 (5457):1433–1438.
Gao Z, Ure K, Ables JL, Lagace DC, Nave KA, Goebbels S, et al. (2009) Neurod1 is essential for the survival and maturation of adult-born neurons. Nat Neurosci 12:1090–1092.
Gleeson JG, Lin PT, Flanagan LA, Walsh CA (1999) Doublecortin is a microtubule-associated protein and is expressed widely by migrating neurons. Neuron 23:257–271.
Gomez-Climent MA, Castillo-Gomez E, Varea E, Guirado R, Blasco-Ibanez JM, Crespo C, et al. (2008) A population of prenatally generated cells in the rat paleocortex maintains an immature neuronal phenotype into adulthood. Cereb Cortex 18:2229–2240.
Gould E, Reeves AJ, Graziano MS, Gross CG (1999) Neurogenesis in the neocortex of adult primates. Science 286(5439):548–552.
Gould E, Vail N, Wagers M, Gross CG (2001) Adult-generated hippocampal and neocortical neurons in macaques have a transient existence. Proc Natl Acad Sci USA 98:10910–10917.
Guo FZ, Ma J, McCauley E, Bannerman P, Pleasure D (2009) Early postnatal proteolipid promoter-expressing progenitors produce multilineage cells *in vivo*. J Neurosci 29:7256–7270.
Guo F, Maeda Y, Ma J, Xu J, Horiuchi M, Miers L, et al. (2010) Pyramidal neurons are generated from oligodendroglial progenitor cells in adult piriform cortex. J Neurosci 30:12036–12049.
Guirado R, Sanchez-Matarredona D, Varea E, Crespo C, Blasco-Ibanez JM, Nacher J (2012) Chronic fluoxetine treatment in middle-aged rats induces changes in the expression of plasticity-related molecules and in neurogenesis. BMC Neurosci 13:5.
Hardingham GE, Cruzalegui FH, Chawla S, Bading H (1998) Mechanisms controlling gene expression by nuclear calcium signals. Cell Calcium 23:131–134.
Hayes NL, Nowakowski RS (2000) Exploiting the dynamics of S-phase tracers in developing brain: interkinetic nuclear migration for cells entering versus leaving the S-phase. Dev Neurosci-Basel 22:44–55.
Hirai T, Yoneda Y (2005) Transcriptional regulation of neuronal genes and its effect on neural functions: gene expression in response to static magnetism in cultured rat hippocampal neurons. J Pharmacol Sci 98:219–224.
Hirai T, Taniura H, Goto Y, Tamaki K, Oikawa H, Kambe Y (2005) Counteraction by repetitive daily exposure to static magnetism against sustained blockade of n-methyl-d-aspartate receptor channels in cultured rat hippocampal neurons. J Neurosci Res 80:491–500.
Hoglinger GU, Rizk P, Muriel MP, Duyckaerts C, Oertel WH, Caille I, et al. (2004) Dopamine depletion impairs precursor cell proliferation in Parkinson's disease. Nat Neurosci 7:726–735.
Homman-Ludiye J, Merson TD, Bourne JA (2012) The early postnatal nonhuman primate neocortex contains self-renewing multipotent neural progenitor cells. PLoS One 7. https://doi.org/10.1371/journal.pone.0034383 e34383.
Huttner HB, Bergmann O, Salehpour M, Racz A, Tatarishvili J, Lindgren E, et al. (2014) The age and genomic integrity of neurons after cortical stroke in humans. Nat Neurosci 17:801–803.
Ince-Dunn G, Hall BJ, Hu SC, Ripley B, Huganir RL, Olson JM, et al. (2006) Regulation of thalamocortical patterning and synaptic maturation by NeuroD2. Neuron 49:683–695.
Inta D, Alfonso J, von Engelhardt J, Kreuzberg MM, Meyer AH, van Hooft JA, et al. (2008) Neurogenesis and widespread forebrain migration of distinct GABAergic neurons from the postnatal subventricular zone. Proc Natl Acad Sci USA 105:20994–20999.
Jin K, Wang X, Xie L, Mao XO, Zhu W, Wang Y, et al. (2006) Evidence for stroke-induced neurogenesis in the human brain. Proc Natl Acad Sci USA 103:13198–13202.

Jin K, Minami M, Lan JQ, Mao XO, Batteur S, Simon RP, et al. (2001) Neurogenesis in dentate subgranular zone and rostral subventricular zone after focal cerebral ischemia in the rat. Proc Natl Acad Sci USA 98:4710–4715.

Jin K, Sun Y, Xie L, Peel A, Mao XO, Batteur S, et al. (2003) Directed migration of neuronal precursors into the ischemic cerebral cortex and striatum. Mol Cell Neurosci 24:171–189.

Kandasamy M, Rosskopf M, Wagner K, Klein B, Couillard-Despres S, Reitsamer HA, et al. (2015) Reduction in subventricular zone-derived olfactory bulb neurogenesis in a rat model of Huntington's disease is accompanied by striatal invasion of neuroblasts. PLoS One 10. https://doi.org/10.1371/journal.pone.0116069 e0116069.

Kang SH, Fukaya M, Yang JK, Rothstein JD, Bergles DE (2010) NG2 + CNS glial progenitors remain committed to the oligodendrocyte lineage in postnatal life and following neurodegeneration. Neuron 68:668–681.

Kaplan MS (1981) Neurogenesis in the 3-month-old rat visual cortex. J Comp Neurol 195:323–338.

Kazanis I (2012) Can adult neural stem cells create new brains? Plasticity in the adult mammalian neurogenic niches: realities and expectations in the era of regenerative biology. Neuroscientist 18:15–27.

Kheifets LI, Afifi AA, Buffler PA, Zhang ZW (1995) Occupational electric and magnetic field exposure and brain cancer: a meta-analysis. J Occup Environ Med 37:1327–1341.

Kim EJ, Ables JL, Dickel LK, Eisch AJ, Johnson JE (2011) Ascl1 (Mash1) defines cells with long-term neurogenic potential in subgranular and subventricular zones in adult mouse brain. PLoS One 6. https://doi.org/10.1371/journal.pone.0018472 e18472.

Klempin F, Kronenberg G, Cheung G, Kettenmann H, Kempermann G (2011) Properties of doublecortin-(DCX)-expressing cells in the piriform cortex compared to the neurogenic dentate gyrus of adult mice. PLoS One 6(10). https://doi.org/10.1371/journal.pone.0025760 e25760.

Koketsu D, Mikami A, Miyamoto Y, Hisatsune T (2003) Nonrenewal of neurons in the cerebral neocortex of adult macaque monkeys. J Neurosci 23:937–942.

Kornack DR, Rakic P (2001) Cell proliferation without neurogenesis in adult primate neocortex. Science 294(5549):2127–2130.

Leone L, Fusco S, Mastrodonato A, Piacentini R, Barbati SA, Zaffina S, et al. (2014) Epigenetic modulation of adult hippocampal neurogenesis by extremely low-frequency electromagnetic fields. Mol Neurobiol 49:1472–1486.

Livak KJ, Schmittgen TD (2001) Analysis of relative gene expression data using real-time quantitative PCR and the 2(-Delta Delta C(T)) method. Methods 25:402–408.

Luzzati F, Bonfanti L, Fasolo A, Peretto P (2009) DCX and PSA-NCAM expression identifies a population of neurons preferentially distributed in associative areas of different pallial derivatives and vertebrate species. Cereb Cortex 19:1028–1041.

Luzzati F, De Marchis S, Fasolo A, Peretto P (2006) Neurogenesis in the caudate nucleus of the adult rabbit. J Neurosci 26:609–621.

Ma Q, Chen C, Deng P, Zhu G, Lin M, Zhang L, et al. (2016) Extremely low-frequency electromagnetic fields promote in vitro neuronal differentiation and neurite outgrowth of embryonic neural stem cells via up-regulating TRPC1. PLoS One 11. https://doi.org/10.1371/journal.pone.0150923 e0150923.

Ma Q, Deng P, Zhu G, Liu C, Zhang L, Zhou Z, et al. (2014) Extremely low-frequency electromagnetic fields affect transcript levels of neuronal differentiation-related genes in embryonic neural stem cells. PLoS One 9(3). https://doi.org/10.1371/journal.pone.0150923 e90041.

Mastrodonato A, Barbati SA, Leone L, Colussi C, Gironi K, Rinaudo M, et al. (2018). Sci Rep 8:262. https://doi.org/10.1038/s41598-017-18676-1.

Macas J, Nern C, Plate KH, Momma S (2006) Increased generation of neuronal progenitors after ischemic injury in the aged adult human forebrain. J Neurosci 26:13114–13119.

Magavi SS, Leavitt BR, Macklis JD (2000) Induction of neurogenesis in the neocortex of adult mice. Nature 405(6789):951–955.

Marti-Fabregas J, Romaguera-Ros M, Gomez-Pinedo U, Martinez-Ramirez S, Jimenez-Xarrie E, Marin R, et al. (2010) Proliferation in the human ipsilateral subventricular zone after ischemic stroke. Neurology 74:357–365.

Malvaut S, Saghatelyan A (2016) The role of adult-born neurons in the constantly changing olfactory bulb network. Neural Plast 2016:1614329. https://doi.org/10.1155/2016/1614329.

Marin-Burgin A, Schinder AF (2012) Requirement of adult-born neurons for hippocampus-dependent learning. Behav Brain Res 227:391–399.

Marxreiter F, Regensburger M, Winkler J (2013) Adult neurogenesis in Parkinson's disease. Cell Mol Life Sci 70:459–473.

Miyakoshi J (2005) Effects of static magnetic fields at the cellular level. Prog Biophys Mol Bio 87:213–223.

Moores CA, Perderiset M, Francis F, Chelly J, Houdusse A, Milligan RA (2004) Mechanism of microtubule stabilization by doublecortin. Mol Cell 14:833–839.

Nacher J, Crespo C, McEwen BS (2001) Doublecortin expression in the adult rat telencephalon. Eur J Neurosci 14:629–644.

Nakamichi N, Ishioka Y, Hirai T, Ozawa S, Tachibana M, Nakamura N, et al. (2009) Possible promotion of neuronal differentiation in fetal rat brain neural progenitor cells after sustained exposure to static magnetism. J Neurosci Res 87:2406–2417.

Nakatomi H, Kuriu T, Okabe S, Yamamoto S, Hatano O, Kawahara N, et al. (2002) Regeneration of hippocampal pyramidal neurons after ischemic brain injury by recruitment of endogenous neural progenitors. Cell 110:429–441.

Nishiyama A, Boshans L, Goncalves CM, Wegrzyn J, Patel KD (2016) Lineage, fate, and fate potential of NG2-glia. Brain Res 1638:116–128.

Ohira K, Furuta T, Hioki H, Nakamura KC, Kuramoto E, Tanaka Y, et al. (2010) Ischemia-induced neurogenesis of neocortical layer 1 progenitor cells. Nat Neurosci 13:173–179.

Oliviero A, Carrasco-López MC, Campolo M, Perez-Borrego YA, Soto-León V, Gonzalez-Rosa JJ (2015) Safety study of transcranial static magnetic field stimulation (tsms) of the human cortex. Brain Stimul 8:481–485.

Olson JM, Asakura A, Snider L, Hawkes R, Strand A, Stoeck J, et al. (2001) NeuroD2 is necessary for development and survival of central nervous system neurons. Dev Biol 234:174–187.

Palmer TD, Markakis EA, Willhoite AR, Safar F, Gage FH (1999) Fibroblast growth factor-2 activates a latent neurogenic program in neural stem cells from diverse regions of the adult CNS. J Neurosci 19:8487–8497.

Parent JM, Valentin VV, Lowenstein DH (2002) Prolonged seizures increase proliferating neuroblasts in the adult rat subventricular zone-olfactory bulb pathway. J Neurosci 22:3174–3188.

Paxinos G, Watson C, Pennisi M, Topple A (1985) Bregma, lambda and the interaural midpoint in stereotaxic surgery with rats of different sex, strain and weight. J Neurosci Meth 13:139–143.

Pekcec A, Loscher W, Potschka H (2006) Neurogenesis in the adult rat piriform cortex. Neuroreport 17:571–574.

Piacentini R, Ripoli C, Mezzogori D, Azzena GB, Grassi C (2008) Extremely low-frequency electromagnetic fields promote in vitro neurogenesis via upregulation of Ca(v)1-channel activity. J Cell Physiol 215:129–139.

Podda MV, Leone L, Barbati SA, Mastrodonato A, Li Puma DD, Piacentini R, et al. (2014) Extremely low-frequency electromagnetic fields enhance the survival of newborn neurons in the mouse hippocampus. Eur J Neurosci 39:893–903.

Ponti G, Peretto P, Bonfanti L (2008) Genesis of neuronal and glial progenitors in the cerebellar cortex of peripuberal and adult rabbits. PLoS One 3. https://doi.org/10.1371/journal.pone.0002366 e2366.

Prasad A, Loong Teh DB, Blasiak A, Chai C, Wu Y, Payam M, et al. (2017) Static magnetic field stimulation enhances oligodendrocyte differentiation and secretion of neurotrophic factors. Scientific Reps. https://doi.org/10.1038/s41598-017-06331-8.

Reynolds BA, Weiss S (1992) Generation of neurons and astrocytes from isolated cells of the adult mammalian central nervous system. Science 255(5052):1707–1710.

Rivers LE, Young KM, Rizzi M, Jamen F, Psachoulia K, Wade A, et al. (2008) PDGFRA/NG2 glia generate myelinating oligodendrocytes and piriform projection neurons in adult mice. Nat Neurosci 11:1392–1401.
Rosen AD (1996) Inhibition of calcium channel activation in GH3 cells by static magnetic fields. Biochim Biophys Acta 1282:149–155.
Rosen AD (2003) Mechanism of action of moderate-intensity static magnetic fields on biological systems. Cell Biochem Biophys 39:163–173.
Ross SE, Greenberg ME, Stiles CD (2003) Basic helix-loop-helix factors in cortical development. Neuron 39:13–25.
Sabelstrom H, Stenudd M, Reu P, Dias DO, Elfineh M, Zdunek S, et al. (2013) Resident neural stem cells restrict tissue damage and neuronal loss after spinal cord injury in mice. Science 342 (6158):637–640.
Saha B, Peron S, Murray K, Jaber M, Gaillard A (2013) Cortical lesion stimulates adult subventricular zone neural progenitor cell proliferation and migration to the site of injury. Stem Cell Res 11:965–977.
Santarelli L, Saxe M, Gross C, Surget A, Battaglia F, Dulawa S, et al. (2003) Requirement of hippocampal neurogenesis for the behavioral effects of antidepressants. Science 301:805–809.
Saunders R (2005) Static magnetic fields: animal studies. Prog Biophys Mol Bio 87:225–239.
Seki T, Arai Y (1991) Expression of highly polysialylated NCAM in the neocortex and piriform cortex of the developing and the adult rat. Anat Embryol 184:395–401.
Shapiro LA, Ng KL, Kinyamu R, Whitaker-Azmitia P, Geisert EE, Blurton-Jones M, et al. (2007) Origin, migration and fate of newly generated neurons in the adult rodent piriform cortex. Brain Struct Funct 212:133–148.
Sun Y, Nadal-Vicens M, Misono S, Lin MZ, Zubiaga A, Hua X, et al. (2001) Neurogenin promotes neurogenesis and inhibits glial differentiation by independent mechanisms. Cell 104:365–376.
Sundholm-Peters NL, Yang HK, Goings GE, Walker A, Szele FG (2005) Subventricular zone neuroblasts emigrate toward cortical lesions. J Neuropath Exp Neur 64:1089–1100.
Tamura Y, Kataoka Y, Cui Y, Takamori Y, Watanabe Y, Yamada H (2007) Multi-directional differentiation of doublecortin- and NG2-immunopositive progenitor cells in the adult rat neocortex in vivo. Eur J Neurosci 25:3489–3498.
Tenuzzo B, Vergallo C, Dini L (2009) Effect of 6mT static magnetic field on the bcl-2, bax, p53 and hsp70 expression in freshly isolated and in vitro aged human lymphocytes. Tissue Cell 41:169–179.
Thomas RM, Hotsenpiller G, Peterson DA (2007) Acute psychosocial stress reduces cell survival in adult hippocampal neurogenesis without altering proliferation. J Neurosci 27:2734–2743.
Tsai PT, Ohab JJ, Kertesz N, Groszer M, Matter C, Gao J, et al. (2006) A critical role of erythropoietin receptor in neurogenesis and post-stroke recovery. J Neurosci 26:1269–1274.
Urban N, Guillemot F (2014) Neurogenesis in the embryonic and adult brain: same regulators, different roles. Front Cell Neurosci 8:396. https://doi.org/10.3389/fncel.2014.00396.
Van den Berge SA, van Strien ME, Korecka JA, Dijkstra AA, Sluijs JA, Kooijman L, et al. (2011) The proliferative capacity of the subventricular zone is maintained in the parkinsonian brain. Brain 134(Pt 11):3249–3263.
Van Praag H, Christie BR, Sejnowski TJ, Gage FH (1999) Running enhances neurogenesis, learning, and long-term potentiation in mice. Proc Natl Acad Sci USA 96:13427–13431.
Vivar C, van Praag H (2013) Functional circuits of new neurons in the dentate gyrus. Front Neural Circuit 7:15. https://doi.org/10.3389/fncir.2013.00015.
West AE, Chen WG, Dalva MB, Dolmetsch RE, Kornhauser JM, Shaywitz AJ, et al. (2001) Calcium regulation of neuronal gene expression. Proc Natl Acad Sci USA 98:11024–11031.
Winner B, Winkler J (2015) Adult neurogenesis in neurodegenerative diseases. CSH Perspect Biol 7(4). https://doi.org/10.1101/cshperspect.a021287 a021287.
Winner B, Kohl Z, Gage FH (2011) Neurodegenerative disease and adult neurogenesis. Eur J Neurosci 33:1139–1151.
Worcester DL (1978) Structural origins of diamagnetic anisotropy in proteins. Proc Natl Acad Sci USA 75:5475–5477.
World Health Organization (WHO). Dementia Fact sheet (2017) http://www.who.int/mediacentre/factsheets/fs362/en/.
Xiong K, Cai Y, Zhang XM, Huang JF, Liu ZY, Fu GM, et al. (2010) Layer I as a putative neurogenic niche in young adult guinea pig cerebrum. Mol Cell Neurosci 45:180–191.
Xiong K, Luo DW, Patrylo PR, Luo XG, Struble RG, Clough RW, et al. (2008) Doublecortin-expressing cells are present in layer II across the adult guinea pig cerebral cortex: partial colocalization with mature interneuron markers. Exp Neurol 211:271–282.
Yamashita T, Ninomiya M, Hernandez Acosta P, Garcia-Verdugo JM, Sunabori T, Sakaguchi M, et al. (2006) Subventricular zone-derived neuroblasts migrate and differentiate into mature neurons in the post-stroke adult striatum. J Neurosci 26:6627–6636.
Yang Y, Xie MX, Li JM, Hu X, Patrylo PR, Luo XG, et al. (2015) Prenatal genesis of layer II doublecortin expressing neurons in neonatal and young adult guinea pig cerebral cortex. Front Neuroanat 9:109. https://doi.org/10.3389/fnana.2015.00109.
Yang Z, Levison SW (2007) Perinatal hypoxic/ischemic brain injury induces persistent production of striatal neurons from subventricular zone progenitors. Dev Neurosci-Basel 29:331–340.
Zhang J, Jiao J (2015) Molecular biomarkers for embryonic and adult neural stem cell and neurogenesis. Biomed Res Int 2015. https://doi.org/10.1155/2015/727542 727542.
Zhao C, Deng W, Gage FH (2008) Mechanisms and functional implications of adult neurogenesis. Cell 132:645–660.
Ziabreva I, Perry E, Perry R, Minger SL, Ekonomou A, Przyborski S, et al. (2006) Altered neurogenesis in Alzheimer's disease. J Psychosom Res 61:311–316.

(Received 11 January 2019, Accepted 4 November 2019)
(Available online 3 December 2019)